

Supplementary Information

Transfer Semi-hydrogenation of Terminal Alkynes with a Well-defined Iron Complex

Deep Chowdhury,^a Souvik Goswami,^a Gamidi Rama Krishna,^b and Arup Mukherjee^{a,*}

^a*Department of Chemistry, Indian Institute of Technology Bhilai, GEC Campus, Sejbahar, Raipur, Chhattisgarh 492015, India*

^b*Centre for X-ray Crystallography, CSIR-National Chemical Laboratory,*

Pune-411008, India

Email: arup@iitbhilai.ac.in

Table of Contents

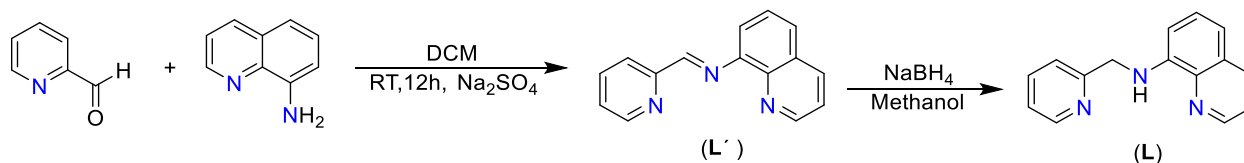
1. General Information
2. Synthesis of the ligand (**L**)
3. Synthesis of the **Fe-1** complex
4. General Procedure for the transfer semi-hydrogenation of terminal alkynes
5. Control studies
6. Monitoring experiment the dehydrogenation of Me₂NH·BH₃ with the ¹¹B NMR spectroscopy
7. General procedure for the detection of H₂ gas during the dehydrogenation of Me₂NH·BH₃ in the presence of **Fe-1** and KO^tBu
8. ¹H and ¹³C{¹H} NMR spectra of the isolated compounds
9. GC Chromatogram of the reaction mixture, peak reports, and mass-spectra of the terminal alkenes
10. Crystallographic information of Fe-1 complex
11. Copies of ¹H and ¹³C{¹H} NMR spectra of the isolated products
12. References

1. General Information:

All chemicals were purchased from Sigma-Aldrich, Alfa-Aesar, Merck, Avra, Loba Chemie, and TCI at the highest purity grade and used for catalytic transfer semi-hydrogenation without further purification. Deuterated solvents were procured from Sigma-Aldrich. Unless otherwise mentioned, all syntheses were performed in standard glassware without any special precautions taken for the removal of moisture or air. NMR spectra were recorded in CDCl_3 and TMS as internal standard on Bruker Avance 400/600 MHz spectrometers. Chemical shifts of ^1H NMR spectra were given in parts per million with respect to TMS and the coupling constant (J) was measured in Hz. The following abbreviations were used to describe the multiplicities: s= singlet, d= doublet, t= triplet, m= multiplet. GC-MS analyses were carried out on a Thermo Scientific Trace 1310 equipped with TG-5SILMS capillary column with ISQ 7000 single quadrupole mass spectrometer. GC analysis was performed on a Thermo Scientific Trace 1310 equipped with a packed column (ShinCarbon ST). High-resolution mass spectrometric analysis was carried out on the Agilent 6546 LC/Q-TOF instrument. UV-Vis studies were carried out on a Shimadzu UV-2600 instrument. FT-IR studies were carried out on a Perkin Elmer instrument.

2. Synthesis of the ligand (L):

The ligand was synthesized according to the reported procedure¹ with some modifications as follows:



Scheme S1. Synthesis of ligand L.

8-aminoquinoline (0.721 g, 5 mmol) was taken in a 100 mL round-bottom flask and dissolved in DCM (30 mL) along with the addition of Na_2SO_4 (~300 mg). To it, 2-pyridinecarboxaldehyde (0.536 g, 5 mmol) was added dropwise. The resulting reaction mixture was stirred for 12 hours at room temperature. After that, the solvent was removed completely under reduced pressure. The resulting yellow oil was dissolved in MeOH (20 mL) and warmed in an oil bath at 45 °C. To it,

excess NaBH₄ (0.757 g, 20 mmol) was added in small portions over a period of one hour, and then the reaction mixture was stirred for another 12 hours under warm conditions. After the evaporation of the solvent completely, the residue was treated with a brine solution and the organic components were extracted with 3 x 50 mL of DCM. The combined organic layers were dried over anhydrous Na₂SO₄. Filtration and evaporation of the solvent yielded the crude product as a brown oil. Further purification was done by column chromatography on silica using EtOAc/hexane as eluent to afford the ligand (**L**) as a thick reddish-brown oil, Yield: 66%.

¹H NMR (400 MHz, CDCl₃): δ 8.79 (d, *J* = 3.3 Hz, 1H), 8.65 (d, *J* = 4.3 Hz, 1H), 8.09 (d, *J* = 8.2 Hz, 1H), 7.69 (t, 1H), 7.46–7.38 (m, 2H), 7.34 (t, *J* = 7.9 Hz, 1H), 7.19 (dd, *J* = 13.9, 7.3 Hz, 1H), 7.09 (d, *J* = 8.1 Hz, 1H), 6.99 (d, *J* = 25.4 Hz, 1H), 6.63 (d, *J* = 7.6 Hz, 1H), 4.74 (s, 2H) ppm.

ESI-mass calculated for [M+H]⁺: 236.1182 , Found: 236.1203.

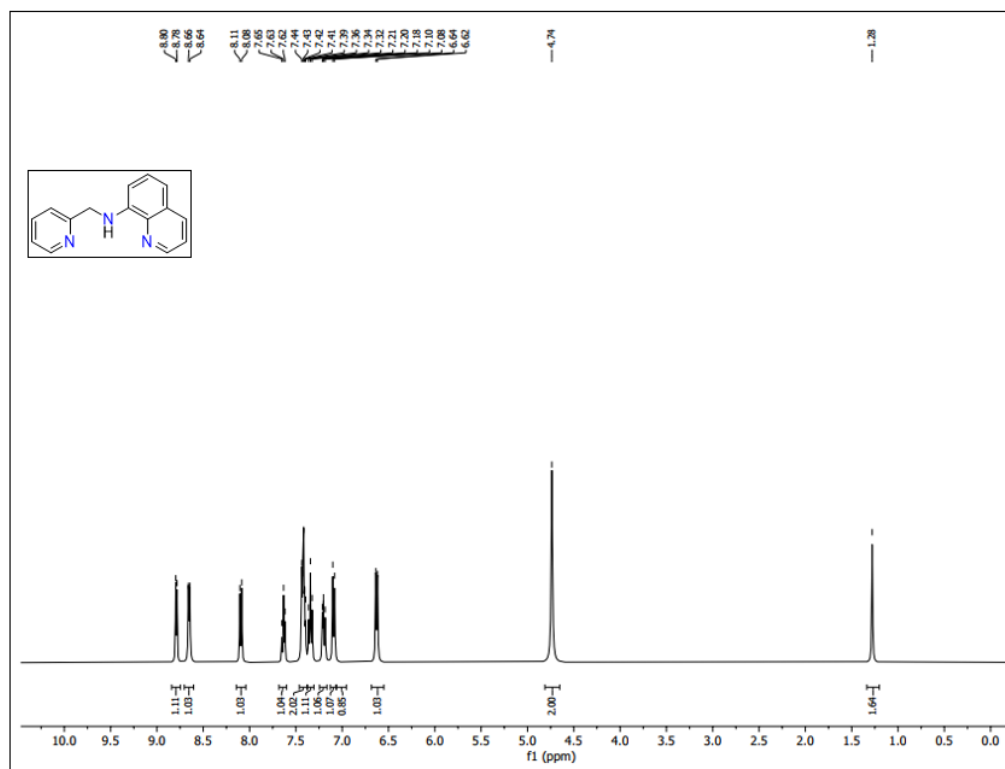
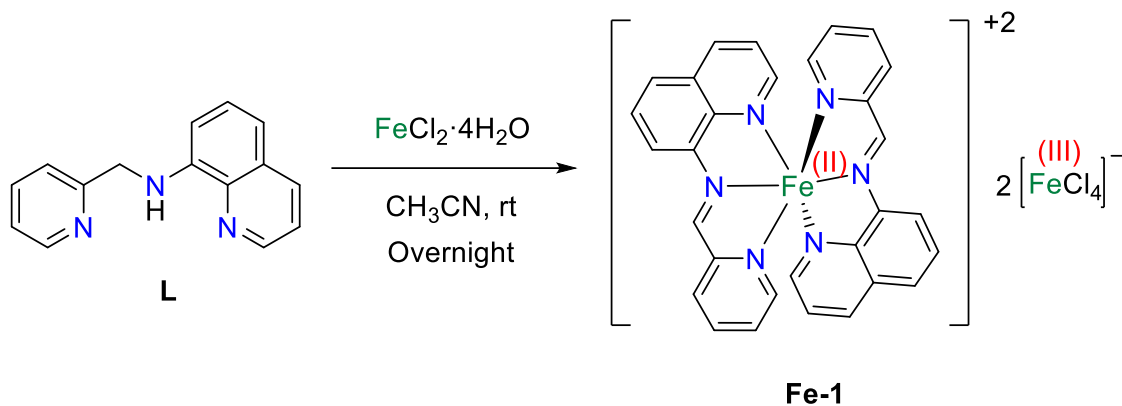


Figure S1. ¹H NMR (400 MHz) spectrum of ligand **L** in CDCl₃.

3. Synthesis of the Fe-1 complex:

Procedure 1.

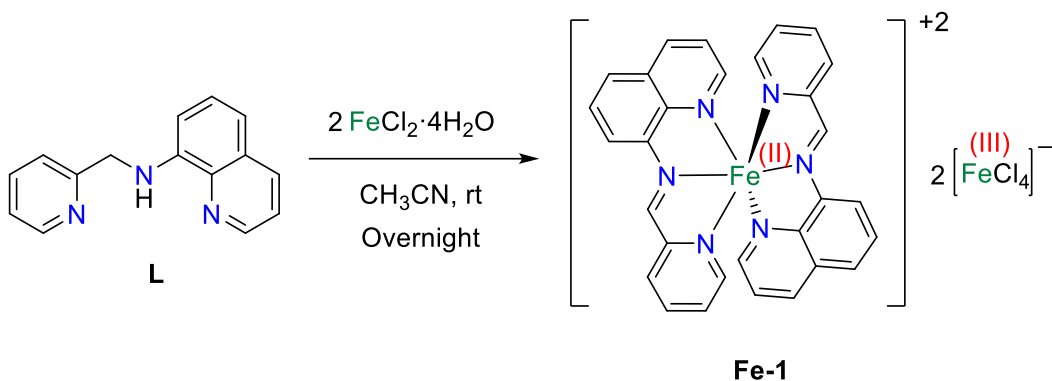
To a solution of **L** (235.3 mg, 1 mmol) in acetonitrile was added $\text{FeCl}_2 \cdot 4\text{H}_2\text{O}$ (198.8 mg, 1 mmol) in a reaction flask. The reaction mixture was stirred overnight under aerobic conditions at room temperature followed by the addition of diethyl ether to obtain a deep green solid. The crude solid was filtered and dried under a vacuum to obtain 161 mg product. Subsequently, the solid was crystallized at room temperature from DCM/hexane solution to obtain the deep green crystals of **Fe-1**, Yield: 70% with respect to $\text{FeCl}_2 \cdot 4\text{H}_2\text{O}$.



Scheme S2a. Synthesis of **Fe-1** complex using 1:1 ligand and metal precursor.

Procedure 2.

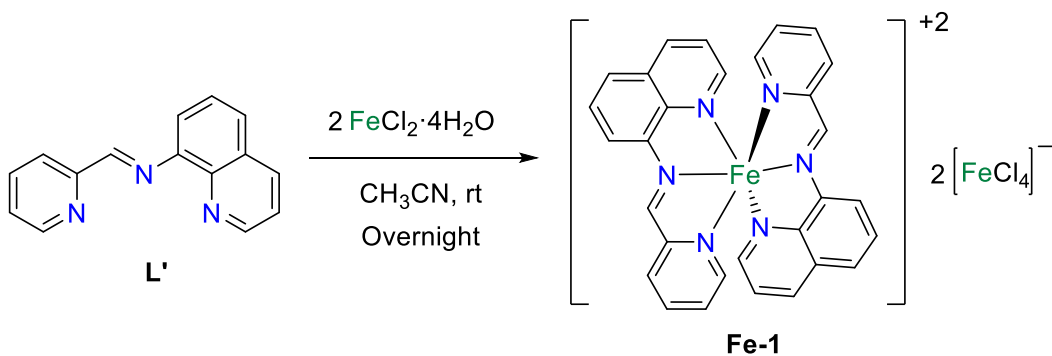
To a solution of **L** (235.3 mg, 1 mmol) in acetonitrile was added $\text{FeCl}_2 \cdot 4\text{H}_2\text{O}$ (387.6 mg, 2 mmol) in a reaction flask. The reaction mixture was stirred overnight under aerobic conditions at room temperature followed by the addition of diethyl ether to obtain a deep green solid. The crude solid was filtered and dried under a vacuum to obtain 358 mg product. Subsequently, the solid was crystallized at room temperature from DCM/hexane solution to obtain the deep green crystals of **Fe-1**, Yield: 78% with respect to ligand (**L**).



Scheme S2b. Synthesis of **Fe-1** complex 1:2 ligand and metal precursor.

Procedure 3.

To a solution of **L'** (235.3 mg, 1 mmol) in acetonitrile was added $\text{FeCl}_2 \cdot 4\text{H}_2\text{O}$ (387.6 mg, 2 mmol) in a reaction flask. The reaction mixture was stirred overnight under aerobic conditions at room temperature followed by the addition of diethyl ether to obtain a deep green solid. The crude solid was filtered and dried under a vacuum to obtain 298.3 mg product. Subsequently, the solid was crystallized at room temperature from DCM/hexane solution to obtain the deep green crystals of **Fe-1**, Yield: 65% with respect to (**L'**).



Scheme S2c. Synthesis of **Fe-1** complex using imine ligand **L'**.

Characterization of Fe-1 complex:

FT-IR (ATR) Spectra: ν (cm^{-1}) = 1595, 1506, 1455, 1595, 1395, 1295, 1204, 1595, 1156, 830, 760.

UV-Vis absorption spectroscopy (methanol): wavelength (nm): 230, 350, 370.

ESI-MS(+): Calculated for $[\text{M}-2\text{FeCl}_4]^{2+}$: 522.1255, Found: 522.1240.

Elemental analysis: Anal. Calcd for $C_{30}H_{22}Cl_8N_6Fe_3$: C, 39.27; H, 2.42; N, 9.16. Found: C, 39.24; H, 2.41; N, 9.18.

(i) IR absorption spectroscopy of Fe-1 complex:

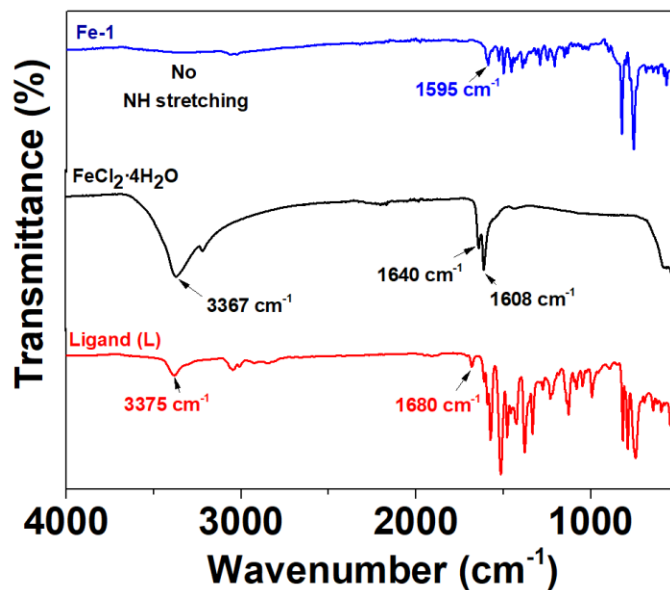


Figure S2. IR absorption spectra of L, $FeCl_2 \cdot 2H_2O$ and Fe-1 complex.

(ii) UV-Vis absorption spectroscopy:

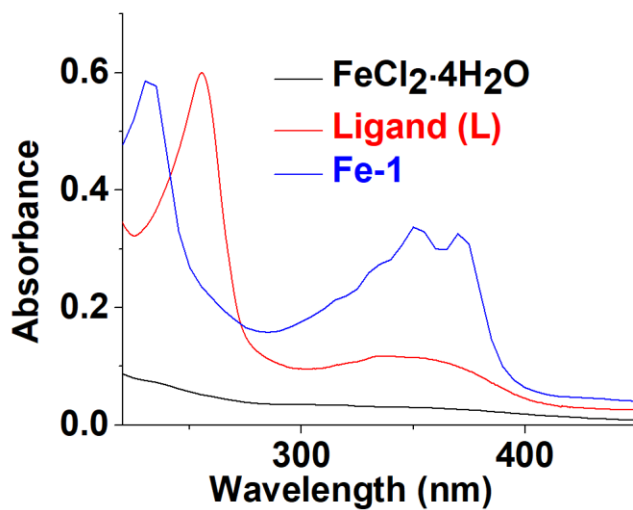


Figure S3. UV-Vis absorption spectra of L, $FeCl_2 \cdot 2H_2O$, and Fe-1 complex in methanol.

(iii) Isotropic Mass distribution:

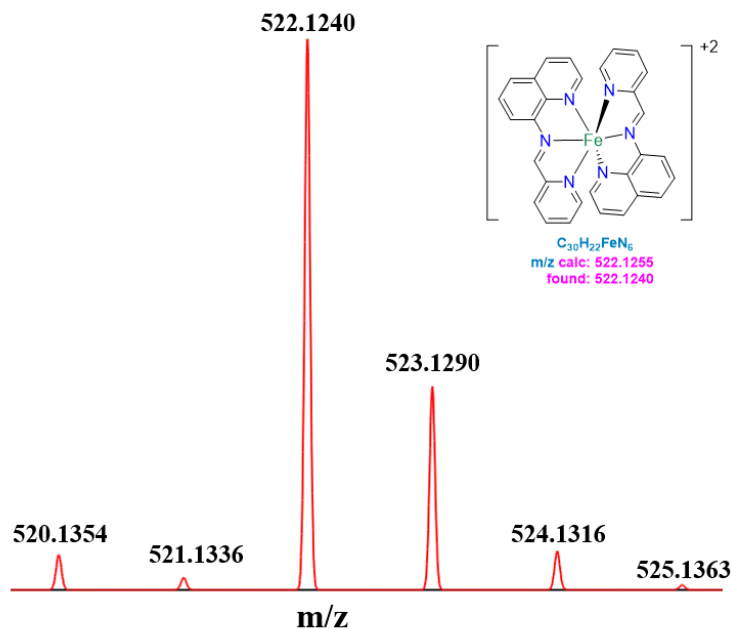


Figure S4. Isotropic Mass distribution of **Fe-1** complex.

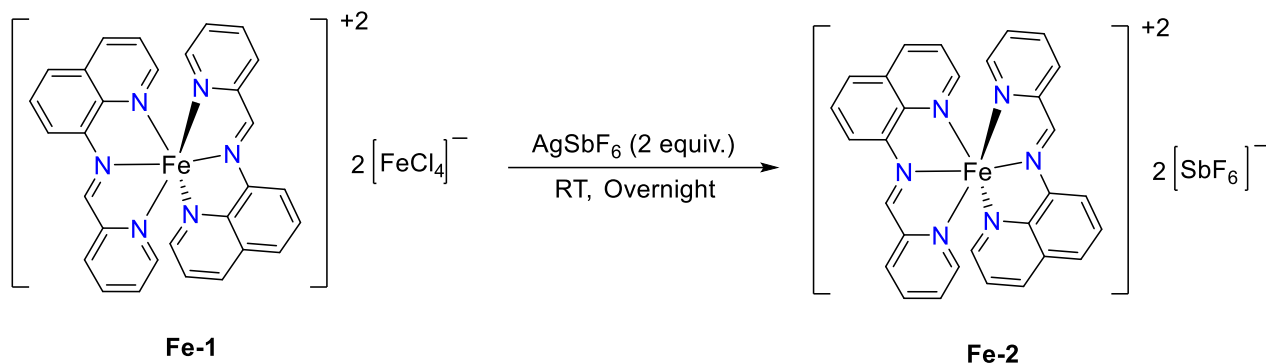
4. General Procedure for the transfer semi-hydrogenation of terminal alkynes:

In a 15 mL thick-wall dry-sealed tube, terminal alkyne (0.2 mmol, 1.0 equiv.), **Fe-1** (0.005 mmol, 1 mol%), KO^tBu (0.005 mmol, 0.01 mmol), and Me₂NH·BH₃ (0.3 mmol, 1.5 equiv.) were dissolved in ⁱPrOH (1 mL) in a N₂ filled glovebox. The tube was sealed tightly with the PTFE screw cap and the resultant reaction mixture was brought outside of the box and kept in a preheated oil bath at 100 °C for 20 h. After completion of the reaction, the mixture was cooled down, opened slowly inside the fume hood, and quenched with the addition of methanol. Following this, 1 equiv. of internal standard (mesitylene) was added to the reaction mixture and a small aliquot was injected in GC-MS to find out the yield of the semi-hydrogenated product. For compounds **2a** and **2b**, the crude reaction mixture was purified through column chromatography using ethyl acetate/hexane as eluent.

CAUTION: Flammable H₂ generated during the reaction. Hence, proper care needs to be taken during the experiment with the reaction vessel.

5. Control Studies:

5a. Procedure for the synthesis of Fe-2 by exchanging the anion of Fe-1 and transfer semi-hydrogenation of phenylacetylene using Fe-2 as a catalyst:



Scheme S3. Exchange of anion of **Fe-1** complex to synthesis **Fe-2** complex.

To a solution of **Fe-1** (1 mmol) in acetonitrile AgSbF_6 (2 mmol) was added to a reaction flask. The reaction mixture was stirred overnight at room temperature followed by the addition of diethyl ether to obtain a deep green solid. The crude solid was filtered and dried under a vacuum to obtain the deep green crystals of **Fe-2**, Yield: 60%.

FT-IR (ATR) Spectra: ν (cm^{-1}) = 1595, 1508, 1455, 1391, 1293, 1210, 1048, 830, 760, 655.

UV-Vis absorption spectroscopy (methanol): wavelength (nm): 233, 352, 374.

ESI-MS(+): Calculated for $[\text{M}+\text{Na}]^+$: 1016.9041, Found: 1016.8995.

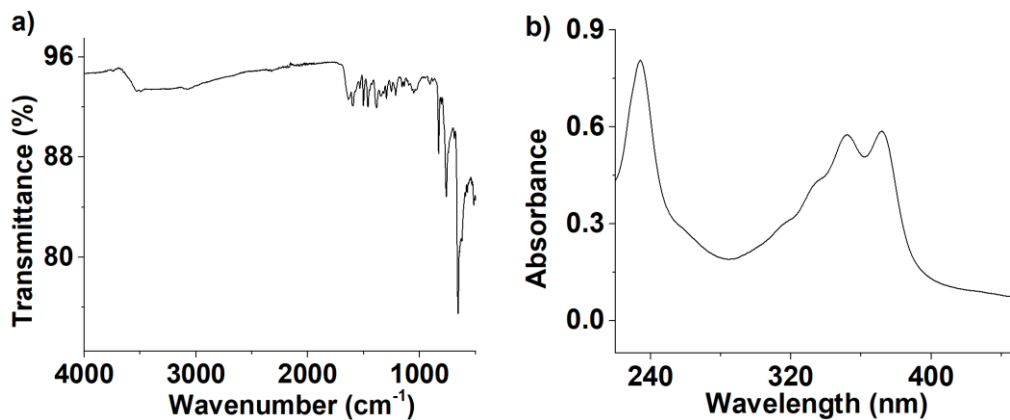
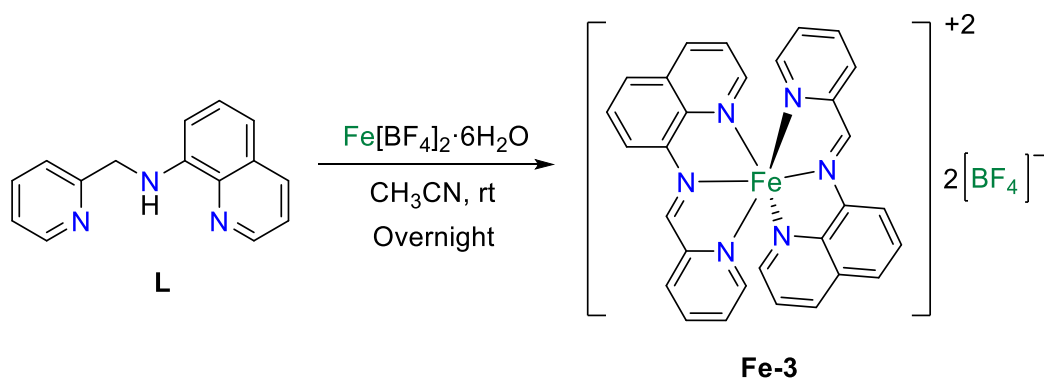


Figure S5. a) IR absorption spectra; b) UV-Vis absorption spectra in methanol of **Fe-2** complex.

Now, in a 15 mL thick-wall dry-sealed tube, phenylacetylene (0.2 mmol, 1.0 equiv.), **Fe-2** (0.005 mmol, 1 mol%), KO^tBu (0.005 mmol, 0.01 mmol), and Me₂NH·BH₃ (0.3 mmol, 1.5 equiv.) were dissolved in ⁱPrOH (1 mL) in a N₂ filled glovebox. The tube was sealed tightly with the PTFE screw cap and the resultant reaction mixture was brought outside of the box and kept in a preheated oil bath at 100 °C for 20 h. After completion of the reaction, the mixture was cooled down, opened slowly inside the fume hood, and quenched with the addition of methanol. Following this, 1 equiv. of internal standard (mesitylene) was added to the reaction mixture and a small aliquot was injected in GC-MS to find out the yield of the semi-hydrogenated product. Yield = 75%

5b. Synthesis of Fe-3 complex and transfer semi-hydrogenation of phenylacetylene using Fe-3 as a catalyst:



Scheme S4. Synthesis of **Fe-3** complex.

To a solution of **L** (1 mmol) in acetonitrile was added FeBF₄·6H₂O (1 mmol) in a reaction flask. The reaction mixture was stirred overnight at room temperature followed by the addition of diethyl ether to obtain a deep green solid. The crude solid was filtered and dried under a vacuum. Subsequently, the solid was crystallized at room temperature from acetonitrile/toluene solution to obtain the deep green crystals of **Fe-3**, Yield: 50%.

¹⁹F NMR: δ -148.38 ppm

FT-IR (ATR) Spectra: ν (cm⁻¹) = 1595, 1504, 1455, 1398, 1293, 1254, 1219, 1048, 830, 516.

UV-Vis absorption spectroscopy (methanol): wavelength (nm): 234, 353, 372.

ESI-MS(+): Calculated for [M+Na]⁺ : 719.1211, Found: 719.1205.

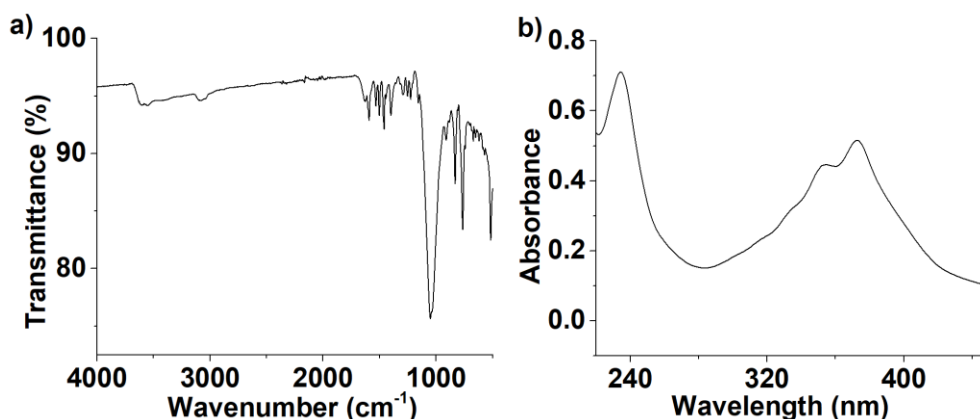
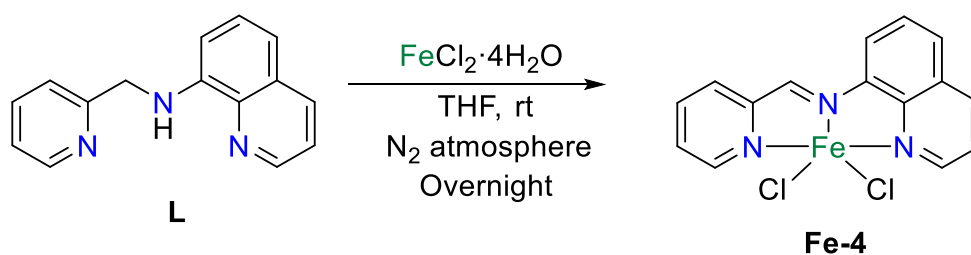


Figure S6. a) IR absorption spectra; b) UV-Vis absorption spectra in methanol of **Fe-3** complex.

Subsequently, in a 15 mL thick-wall dry-sealed tube, phenylacetylene (0.2 mmol, 1.0 equiv.), **Fe-3** (0.005 mmol, 1 mol%), KO^tBu (0.005 mmol, 0.01 mmol), and Me₂NH·BH₃ (0.3 mmol, 1.5 equiv.) were dissolved in ⁱPrOH (1 mL) in a N₂ filled glovebox. The tube was sealed tightly with the PTFE screw cap and the resultant reaction mixture was brought outside of the box and kept in a preheated oil bath at 100 °C for 20 h. After completion of the reaction, the mixture was cooled down, opened slowly inside the fume hood, and quenched with the addition of methanol. Following this, 1 equiv. of internal standard (mesitylene) was added to the reaction mixture and a small aliquot was injected in GC-MS to find out the yield of the semi-hydrogenated product. Yield = 85%

5c. Synthesis of Fe-4 complex using FeCl₂·4H₂O and proligand (L) under N₂ atmosphere.



Scheme S5. synthesize **Fe-4** complex.

To a solution of **L** (235.3 mg, 1 mmol) in THF was added FeCl₂·4H₂O (198.8 mg, 1 mmol) in a reaction flask in an N₂-filled glovebox. The reaction mixture was stirred overnight under the inert condition at room temperature which resulted in the formation of a brownish-red solid

precipitation. The reaction mixture was filtered and washed with diethyl ether to obtain a brownish-red solid. The crude solid was dried under a vacuum to obtain 325 mg product.

FT-IR (ATR) Spectra: ν (cm^{-1}) = 1593, 1500, 1382, 1341, 1285, 1090, 1014, 824, 762, 485.

UV-Vis absorption spectroscopy (methanol): wavelength (nm): 372, 353, 255, 234, 202.

ESI-MS(+): Calculated for $[\text{M}-\text{Cl}]^+$: 323.999, Found: 324.0103.

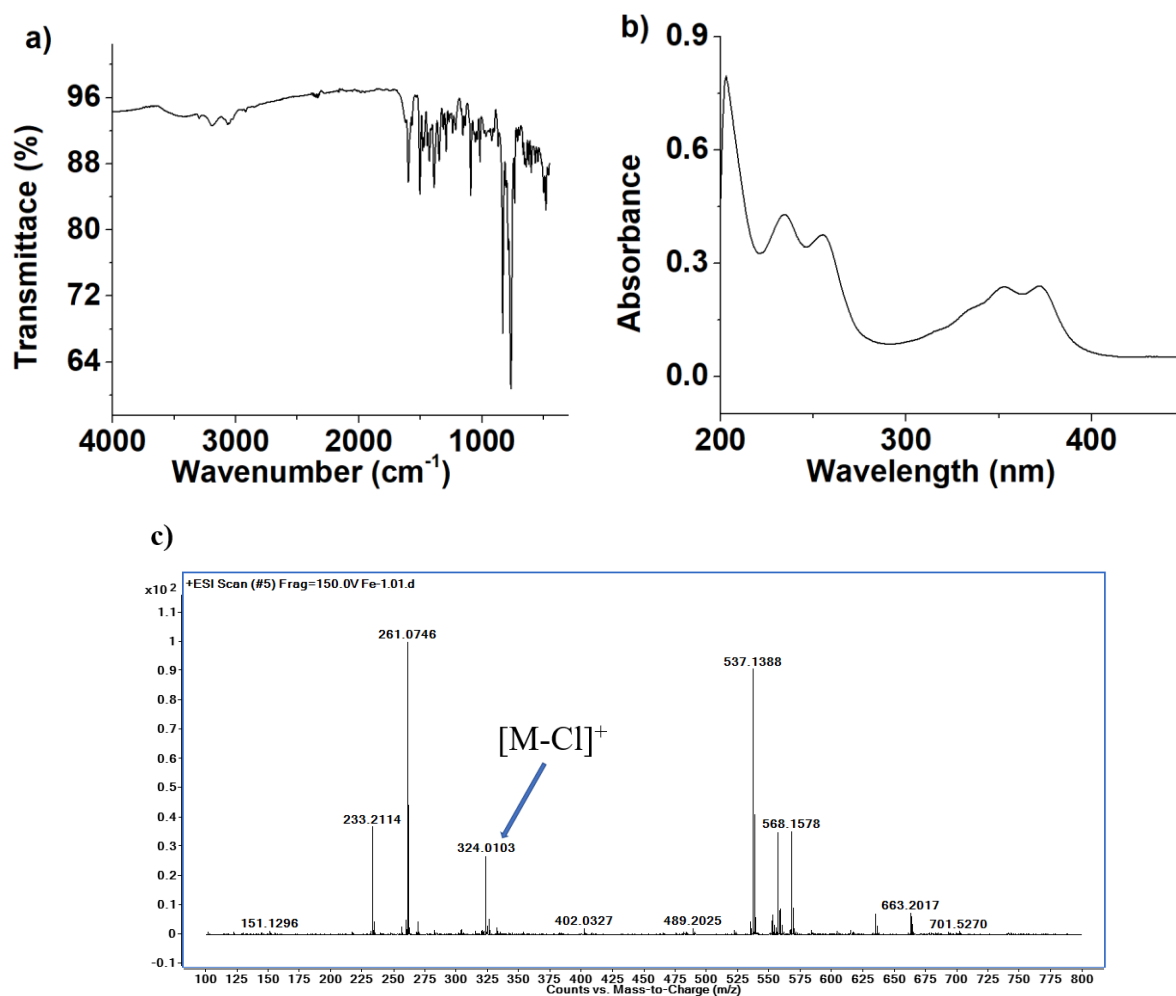
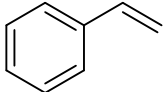
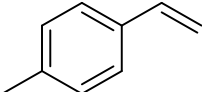
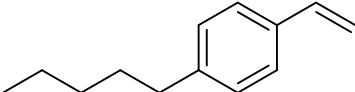
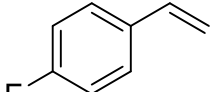
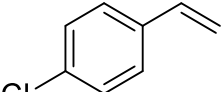
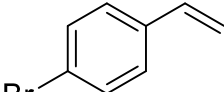
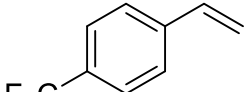
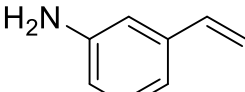
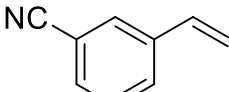
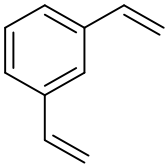
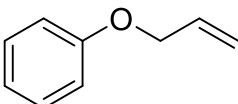
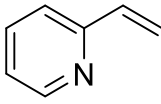
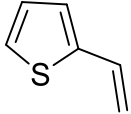


Figure S7. a) IR absorption spectra; b) UV-Vis absorption spectra; c) ESI-MS(+) of the **Fe-4**.

(a) GC-MS data of the alkenes:

The data is based on the measurement of the sample in Thermo-Fisher Trace 1310 GC Chromatography and ISQ 7000 single quadrupole mass spectrometer equipped with TG-5SILMS capillary column and He as carrier gas with flow rate of 1 mL/minute.

 $t_r = 3.6 \text{ min}$ $m/z = 104.11$	 $t_r = 4.06 \text{ min}$ $m/z = 118.14$	 $t_r = 7.27 \text{ min}$ $m/z = 175.20$
 $t_r = 3.10 \text{ min}$ $m/z = 122.08$	 $t_r = 4.78 \text{ min}$ $m/z = 140.07$	 $t_r = 5.57 \text{ min}$ $m/z = 184.02$
 $t_r = 3.27 \text{ min}$ $m/z = 172.08$	 $t_r = 5.99 \text{ min}$ $m/z = 120.15$	 $t_r = 5.99 \text{ min}$ $m/z = 129.04$
 $t_r = 5.11 \text{ min}$ $m/z = 131.17$	 $t_r = 4.77 \text{ min}$ $m/z = 135.11$	 $t_r = 3.42 \text{ min}$ $m/z = 106.09$

	 <p>$t_r = 3.06 \text{ min}$ $m/z = 110.05$</p>	
--	------------------------------------------------------------------------------------------------------------------------------------------------------------	--

6. Monitoring experiment the dehydrogenation of $\text{Me}_2\text{NH}\cdot\text{BH}_3$ with the ^{11}B NMR spectroscopy:

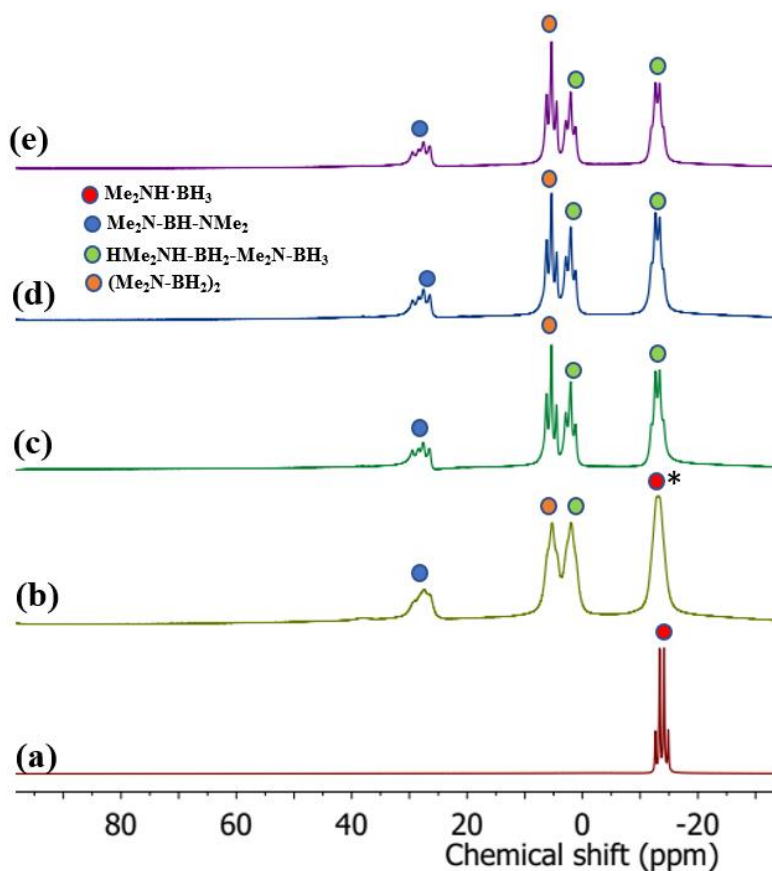
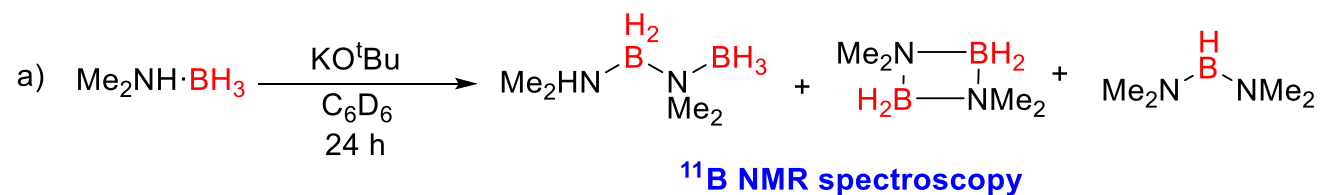


Figure S8. Monitoring by ^{11}B NMR spectroscopy of the reaction between **Fe-1**/ KO^tBu and $\text{Me}_2\text{NH}\cdot\text{BH}_3$ in C_6D_6 : a) DMAB in C_6D_6 ; b) reaction mixture after 0 h; c) reaction mixture after 3 h; d) reaction mixture after 6 h; e) reaction mixture after 24 h; * BH_3 resonance of $\text{HMe}_2\text{NBH}_2\text{Me}_2\text{NBH}_3$ at -13 ppm overlaps with DMAB peak.

In a reaction tube containing Me₂NH·BH₃ (0.5 mmol, 1.5 equiv.), **Fe-1** (1 mol%), KO^tBu (5 mol%) were taken in C₆D₆ under a N₂ filled glove-box and stirred for a few minutes. After that, the reaction mixture was filtered through a syringe, and the filtrate was taken in a screw-cap NMR tube and ¹¹B NMR was measured. Following this, the ¹¹B NMR spectroscopy was recorded after different time intervals (3 h, 6 h and 24 h) to monitor the different boron species generated during the dehydrogenation of Me₂NH·BH₃.



Scheme S6. a) Controlled experiment for disproportionation of Me₂NH·BH₃ mediated by KO^tBu;

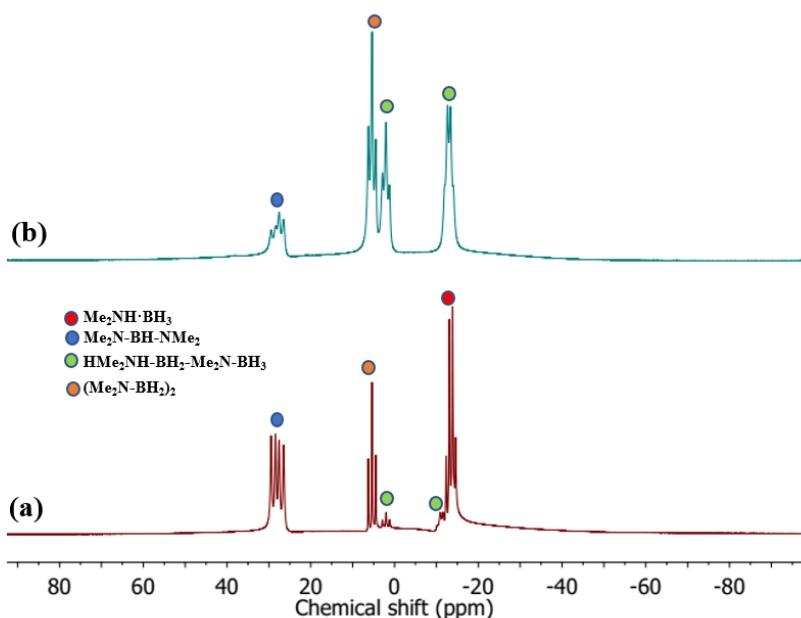


Figure S9. a) The ¹¹B NMR spectroscopy of the reaction between Me₂NH·BH₃ and KO^tBu in C₆D₆ after 24 h; b) The ¹¹B NMR spectroscopy of the reaction between **Fe-1**, KO^tBu, and Me₂NH·BH₃ in C₆D₆ after 24 h.

we have conducted an experiment of Me₂NH·BH₃ and KO^tBu mixing them in 1:1 ratio in the absence of the **Fe-1** (Scheme S6), where we found that even heating the reaction mixture up-to 60 °C, most of the Me₂NH·BH₃ remains unreacted and rest amount is getting disproportionated to Me₂N-

BH-NMe₂ and (Me₂N-BH₂)₂ (Fig. S9) while in presence of catalytic amount **Fe-1** / KO^tBu, Me₂NH·BH₃ undergoes almost full dehydrogenation leading to the formation of (Me₂N-BH₂)₂, Me₂NH-BH₂-Me₂N-BH₃, and Me₂N-BH-NMe₂ during the disproportionation protocol (Fig. S8). This experiment clearly signifies the role of **Fe-1** in observed disproportionation of Me₂NH·BH₃.

7. General procedure for the detection of H₂ gas during the dehydrogenation of Me₂NH·BH₃ in the presence of **Fe-1** and KO^tBu:

An over dried Schlenk tube was charged with Me₂NH·BH₃ (0.5 mmol, 1 equiv.), **Fe-1** (1 mol%) and KO^tBu (5 mol%) in a N₂ filled glove-box. The tube was sealed tightly with septa and the resultant reaction mixture was stirred for 24 h at room temperature. Subsequently, the generated gas in the tube was injected in GC through air tight syringe to find out the evolution of the H₂ gas.

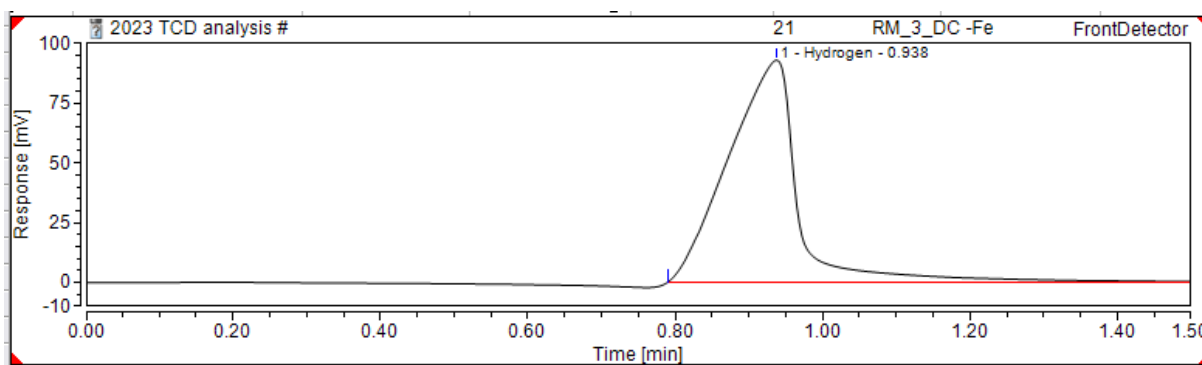
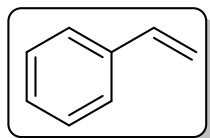


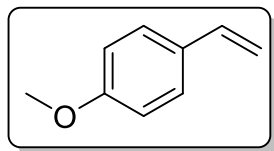
Figure S10. Detection of H₂ gas through the GC in TCD detector for the dehydrogenation of Me₂NH·BH₃ in the presence of **Fe-1**/KO^tBu under neat conditions.

8. ¹H and ¹³C{¹H} NMR Spectra of the Isolated Compounds:

Styrene (2a)²: Isolated yield (17.5 mg, 84%). ¹H NMR (600 MHz, CDCl₃): δ (ppm): 7.29 (dd, *J* = 7.1, 3.3 Hz, 2H), 7.20 (ddd, *J* = 7.6, 6.7, 3.8 Hz, 1H), 7.16-7.12 (m, 1H), 6.61 (m, 1H), 5.64 (m, 1H), 5.13 (ddd, *J* = 10.9, 2.8, 1.8 Hz, 1H); ¹³C{¹H} NMR (125 MHz, CDCl₃): δ (ppm): 137.67, 137.0, 128.61, 127.89, 126.32, 113.87.



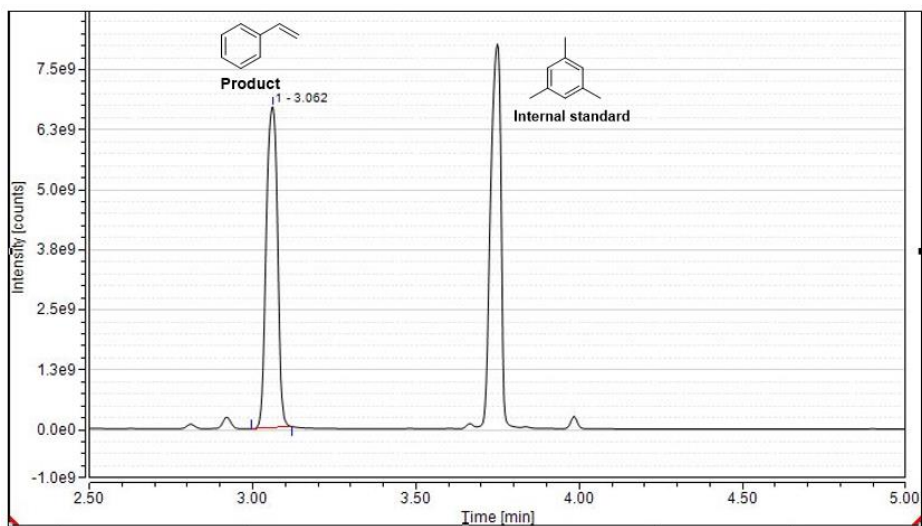
4-vinylanisole (2b)² : Isolated yield (24.5 mg, 91%). ¹H NMR (600 MHz, CDCl₃): δ (ppm): 7.50



(m, 2H), 7.01 (m, 2H), 6.84 (m, 1H), 5.80 (m, 1H), 5.30 (m, 1H), 3.89 (s, 3H); ¹³C{¹H} NMR (125 MHz, CDCl₃): δ (ppm): 159.63, 136.5, 130.589, 127.57, 114.079, 111.57, 55.20.

9. GC Chromatogram of the reaction mixture, peak reports, and mass-spectra of the terminal alkenes

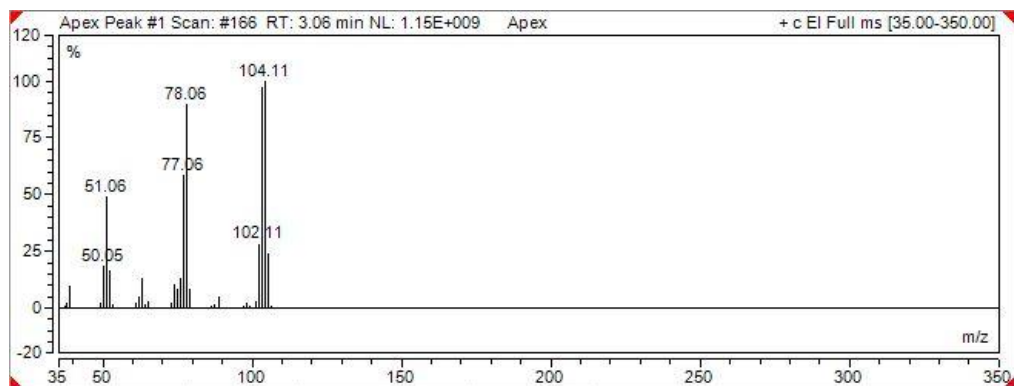
(i) GC Chromatogram of the reaction mixture of compound 2a:



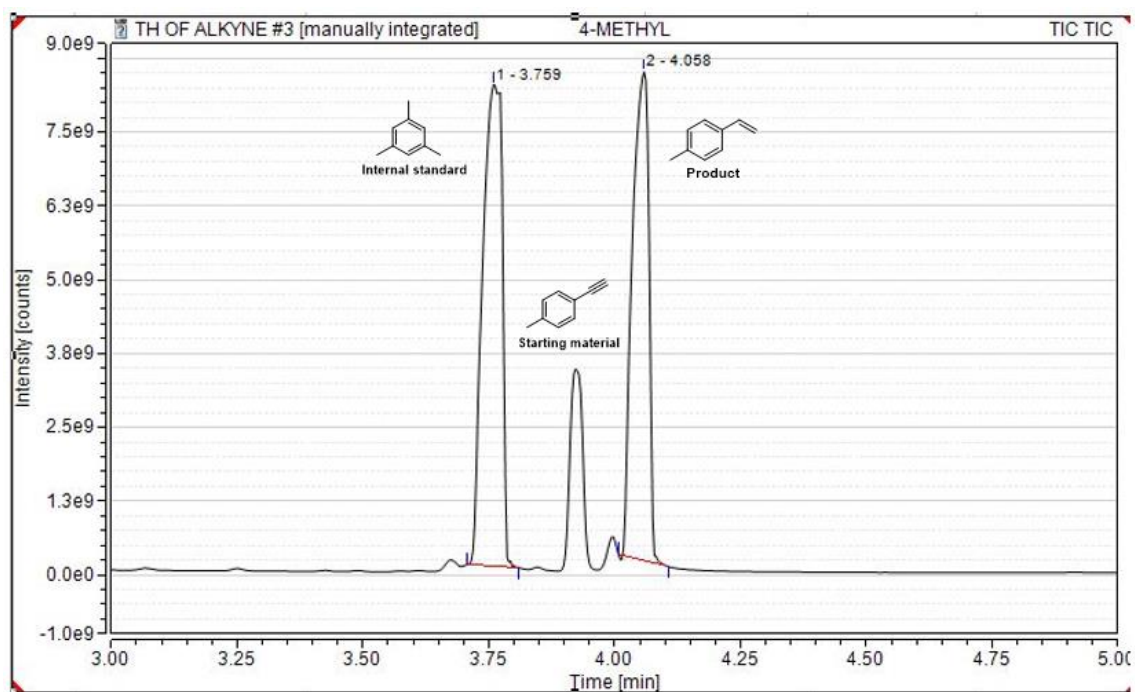
Peak Report

Peak	Retention Time (min)	Peak Area	Name
1	3.06	272551954	Styrene
2	3.77	294106570	Mesitylene

ESI-MS Spectra of styrene



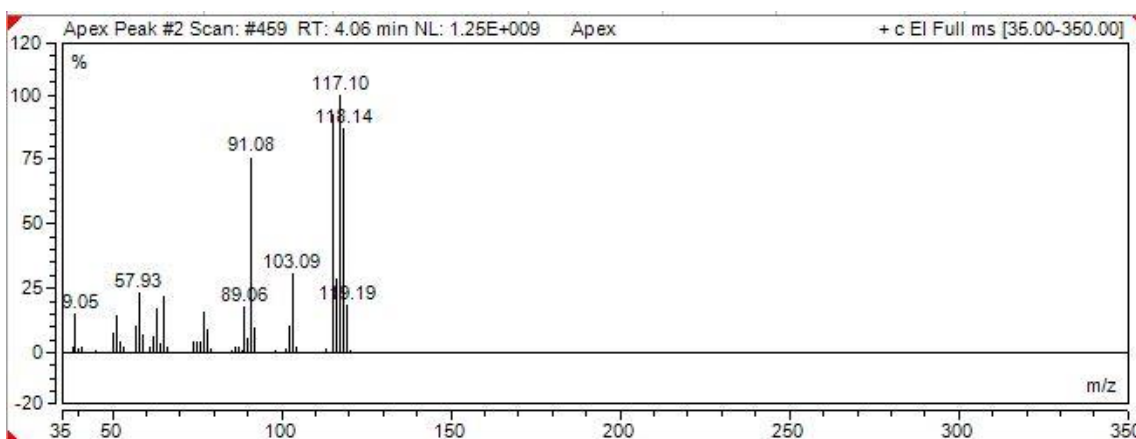
(ii) GC Chromatogram of the reaction mixture of compound 2b:



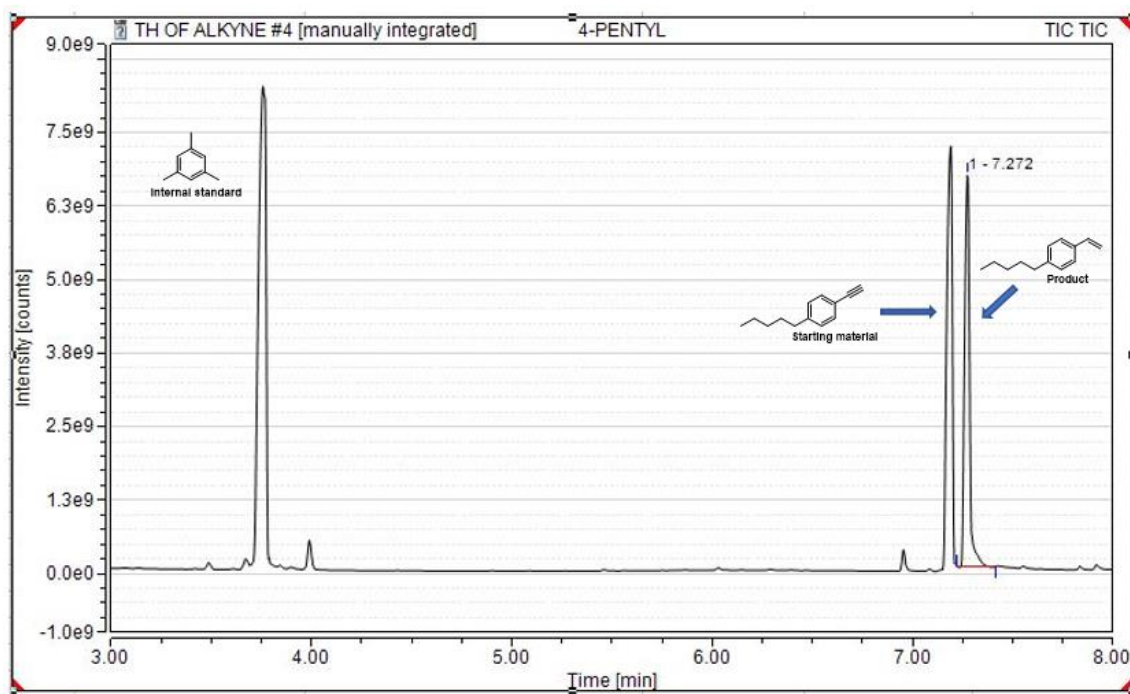
Peak Report

Peak	Retention Time (min)	Peak Area	Name
1	4.06	313555905	4-methylstyrene
2	3.77	365815044	Mesitylene

ESI-MS Spectra of 4-methylstyrene



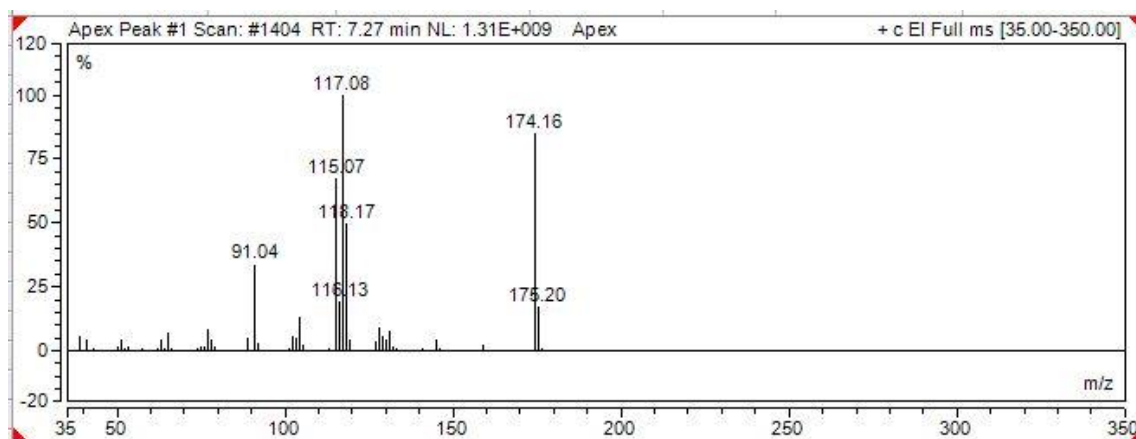
(iii) GC Chromatogram of the reaction mixture of compound 2c:



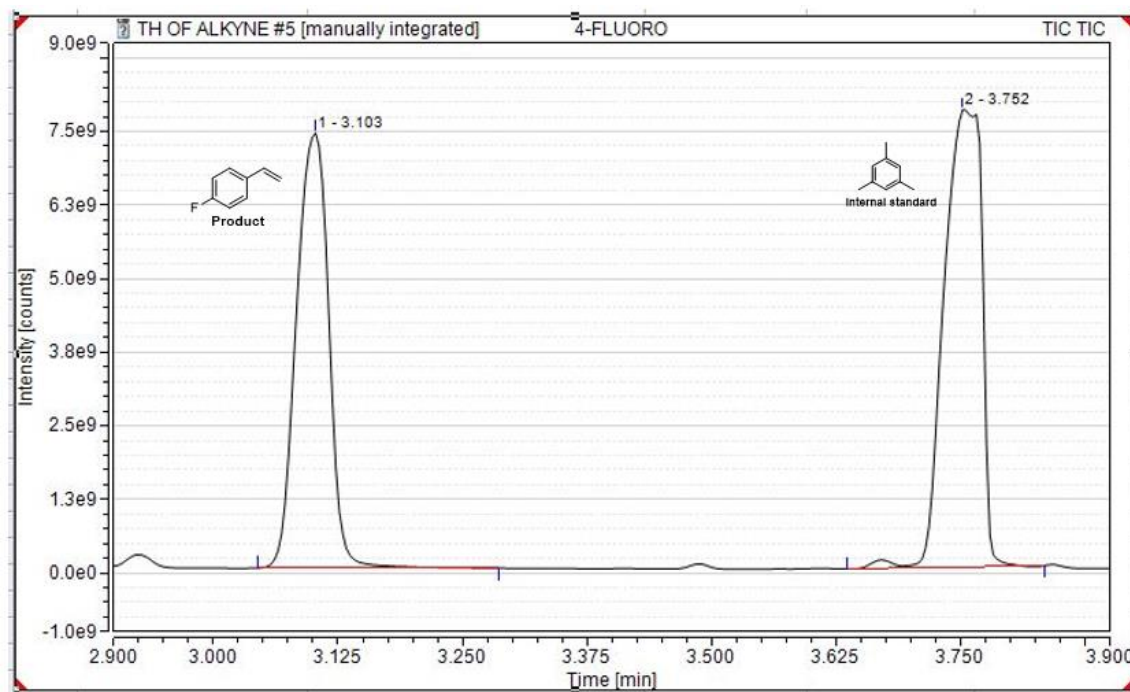
Peak Report

Peak	Retention Time (min)	Peak Area	Name
1	7.27	191747190	4-pentylstyrene
2	3.77	347404193	Mesitylene

ESI-MS Spectra of 4-pentylstyrene



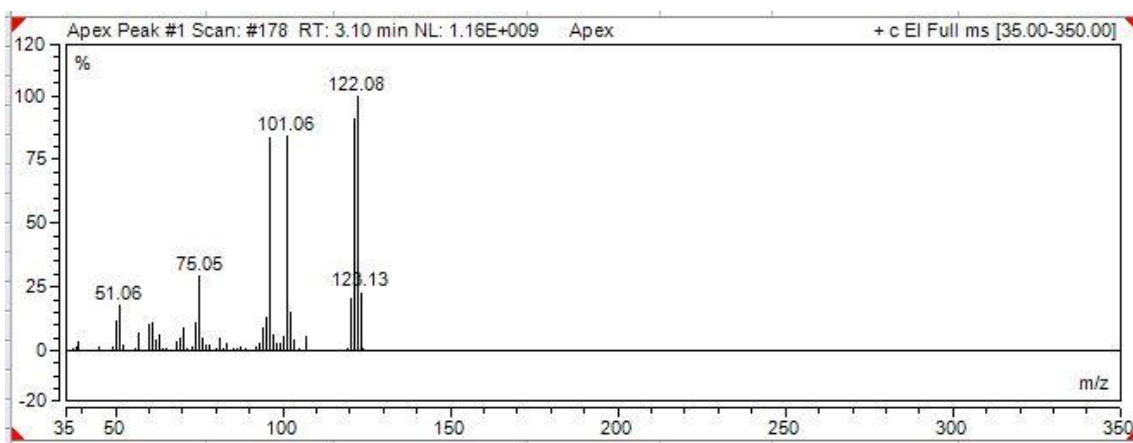
(iv) GC Chromatogram of the reaction mixture of compound 2d:



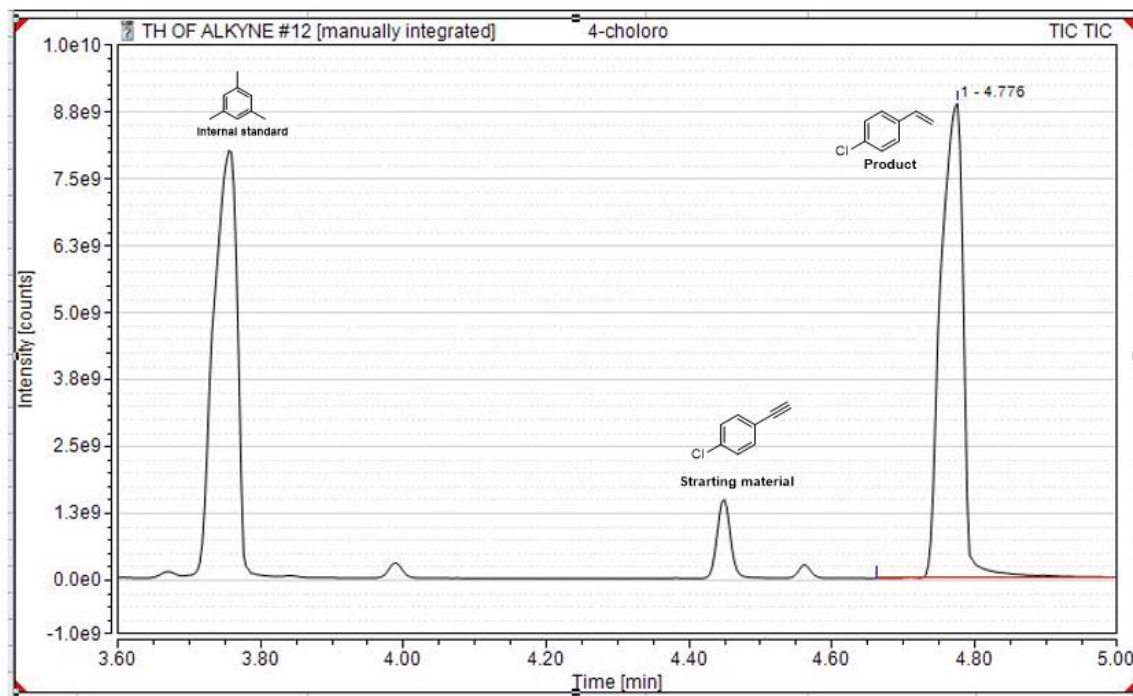
Peak Report

Peak	Retention Time (min)	Peak Area	Name
1	3.10	277718812	4-fluorostyrene
2	3.77	341200258	Mesitylene

ESI-MS Spectra of 4-fluorostyrene



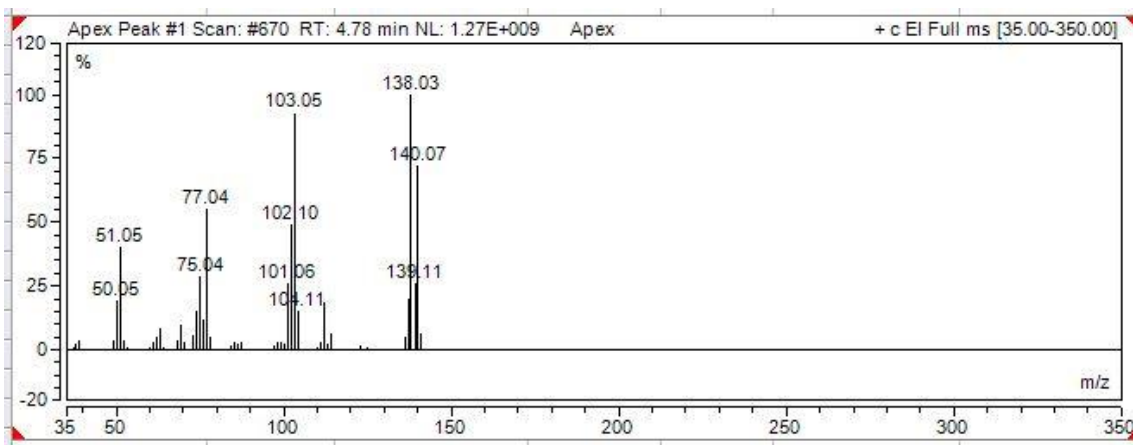
(v) GC Chromatogram of the reaction mixture of compound 2e:



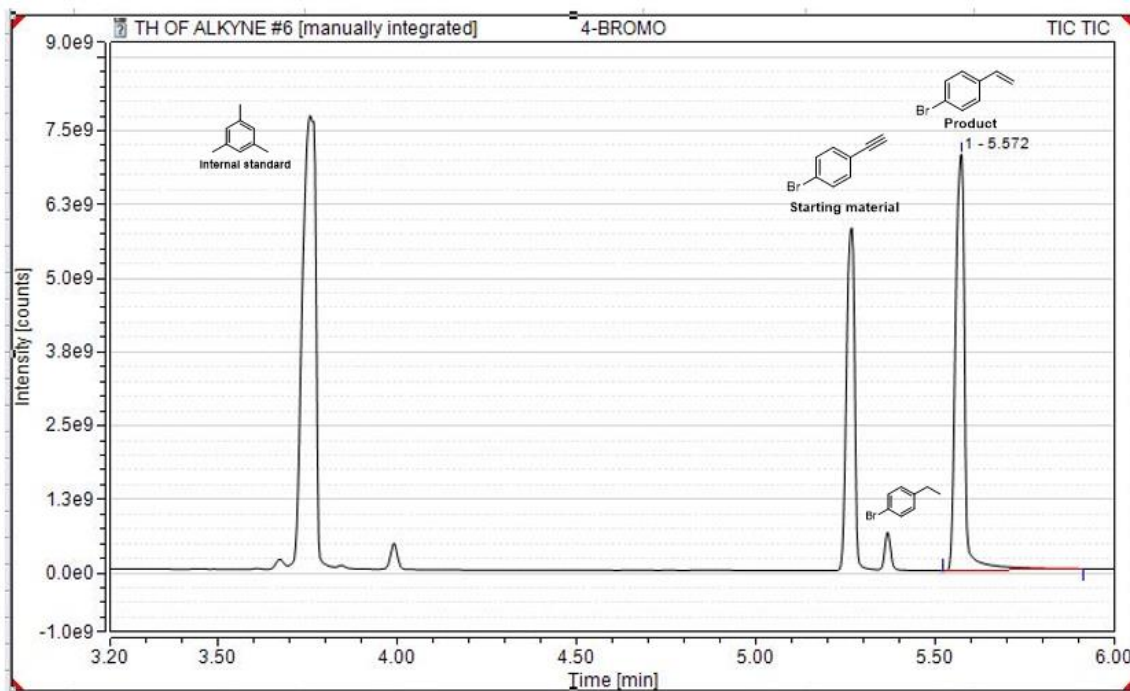
Peak Report

Peak	Retention Time (min)	Peak Area	Name
1	4.78	302826347	4-chlorostyrene
2	3.77	293143999	Mesitylene

ESI-MS Spectra of 4-chlorostyrene



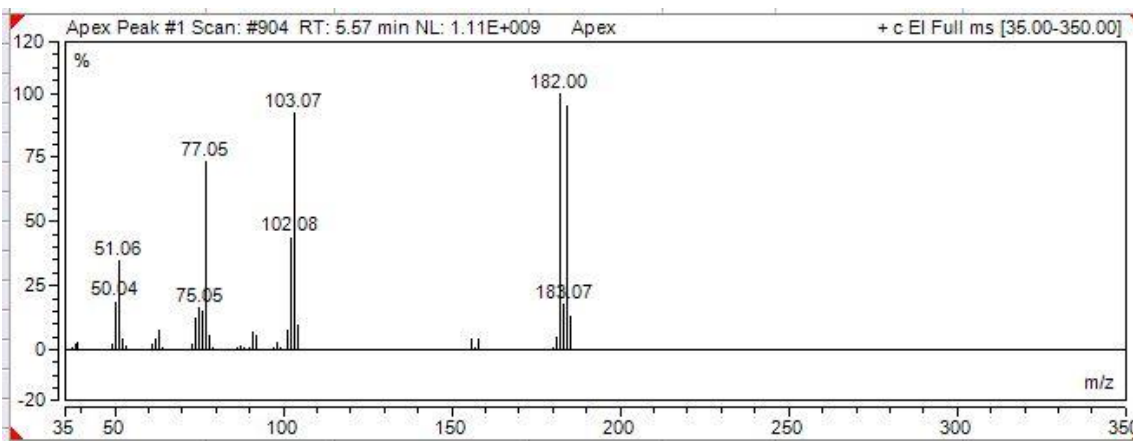
(vi) GC Chromatogram of the reaction mixture of compound 2f:



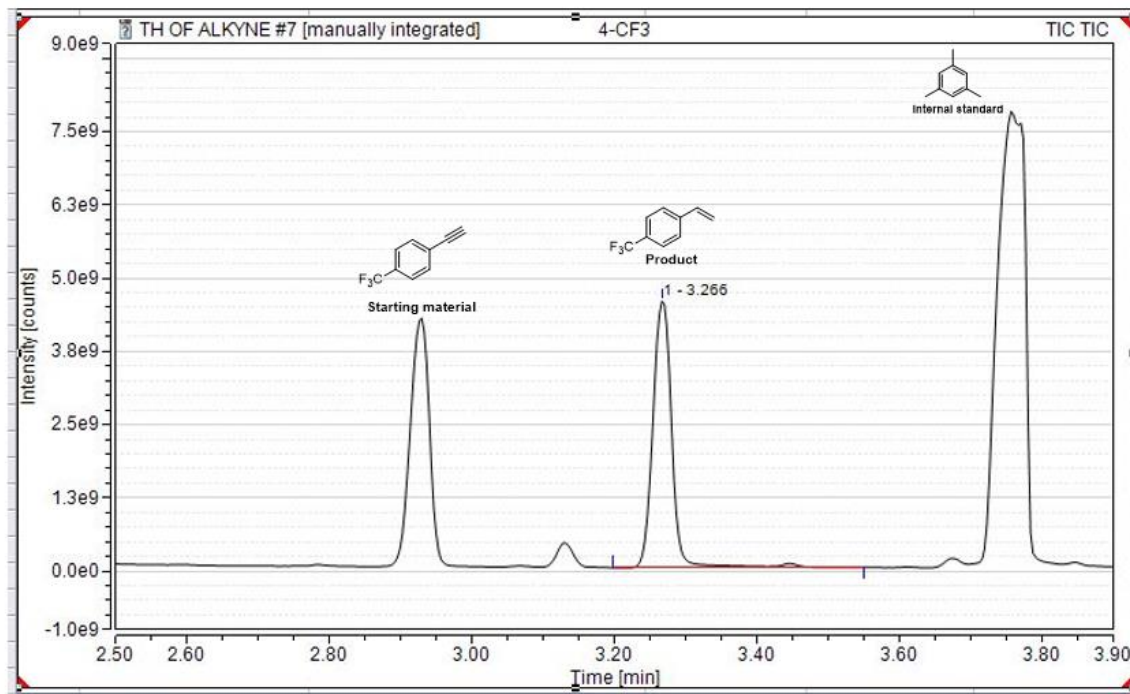
Peak Report

Peak	Retention Time (min)	Peak Area	Name
1	5.57	213939314	4-bromostyrene
2	3.77	318233497	Mesitylene

ESI-MS Spectra of 4-bromostyrene



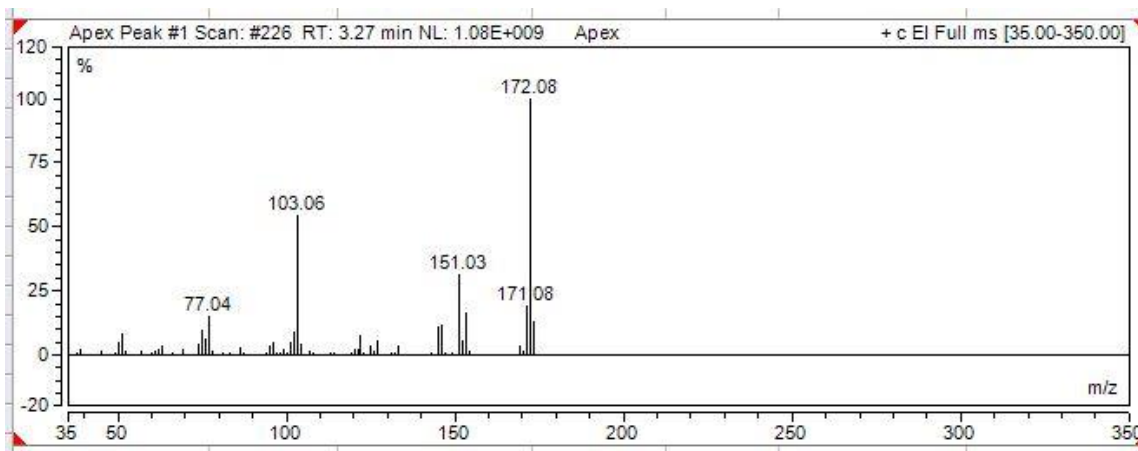
(vii) GC Chromatogram of the reaction mixture of compound 2g:



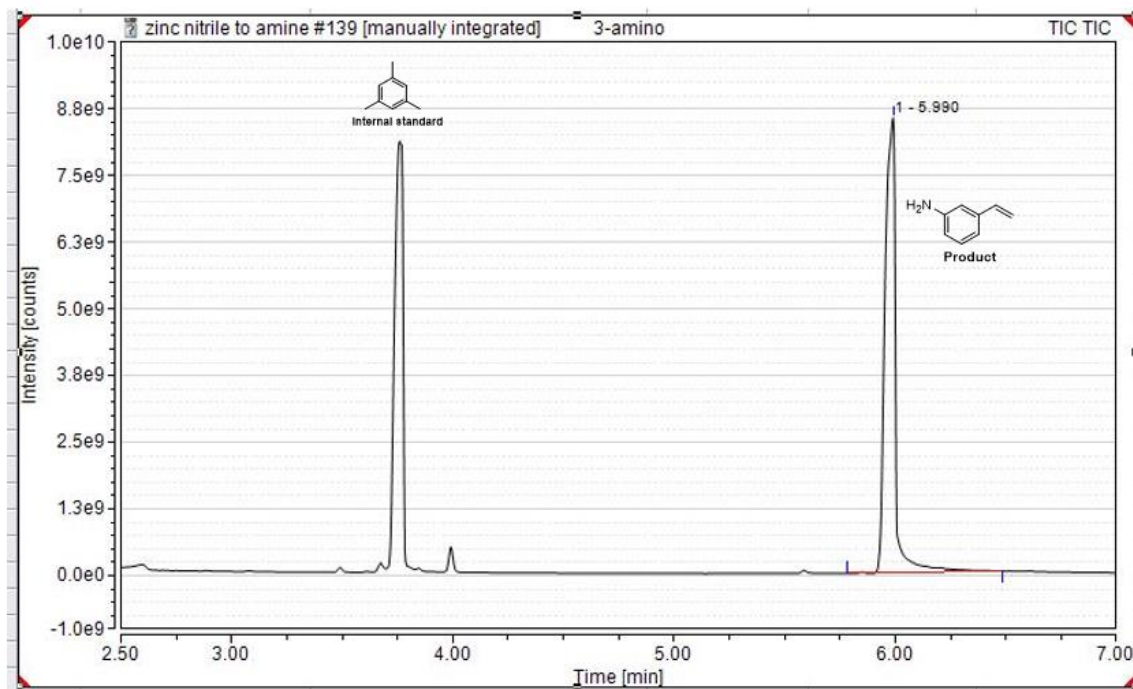
Peak Report

Peak	Retention Time (min)	Peak Area	Name
1	3.27	137492651	4-(Trifluoromethyl)styrene
2	3.77	334108220	Mesitylene

ESI-MS Spectra of 4-(Trifluoromethyl)styrene



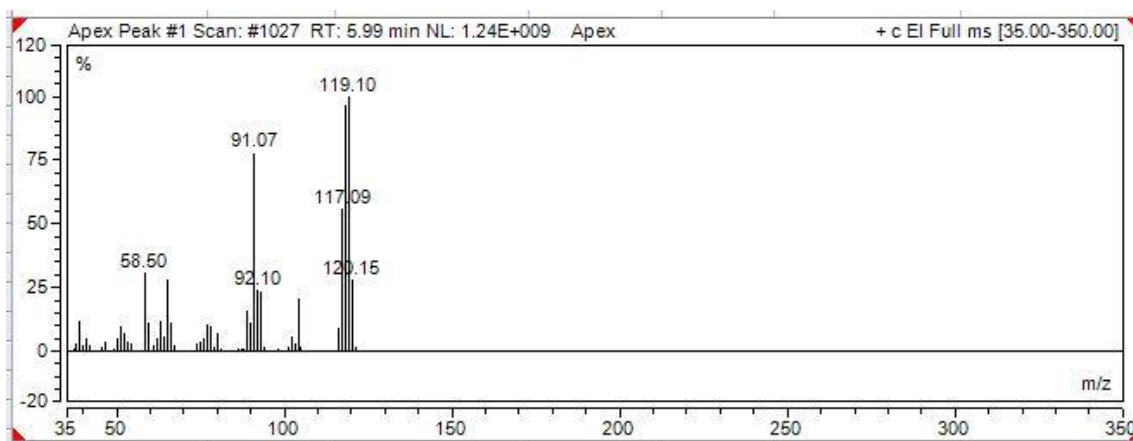
(viii) GC Chromatogram of the reaction mixture of compound 2h:



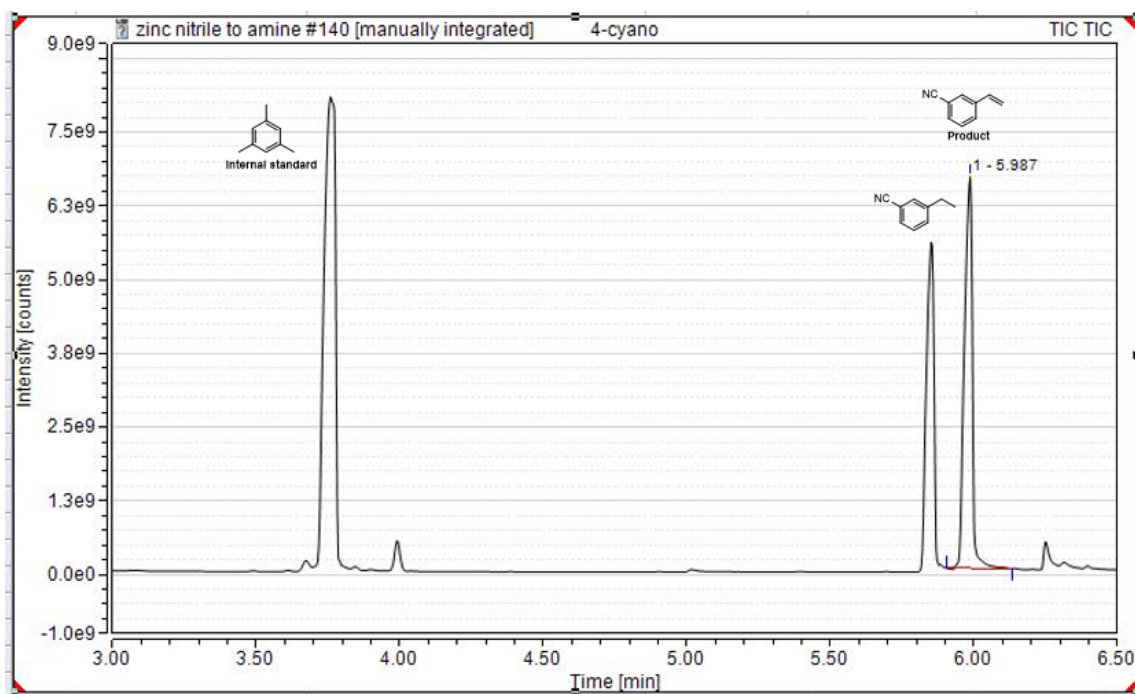
Peak Report

Peak	Retention Time (min)	Peak Area	Name
1	5.99	402698984	3-vinylaniline
2	3.77	342434800	Mesitylene

ESI-MS Spectra of 3-vinylaniline



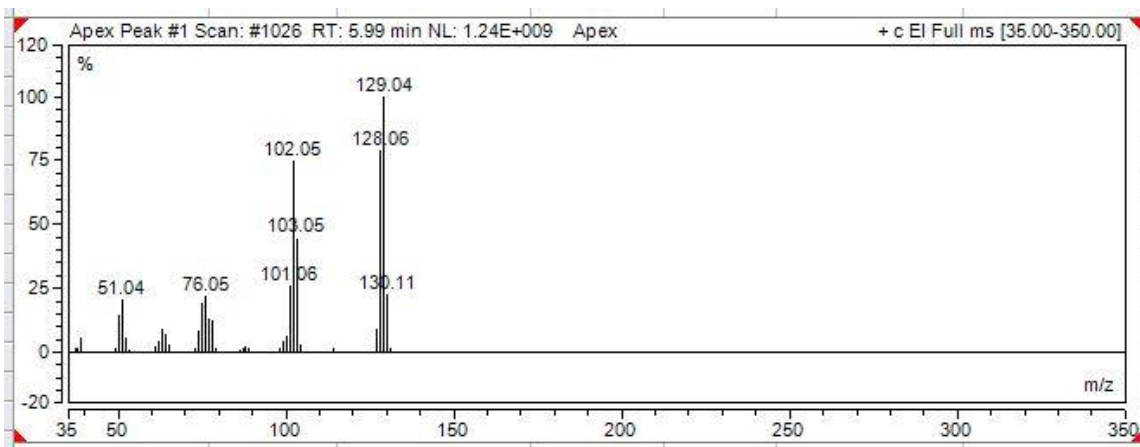
(ix) GC Chromatogram of the reaction mixture of compound 2i:



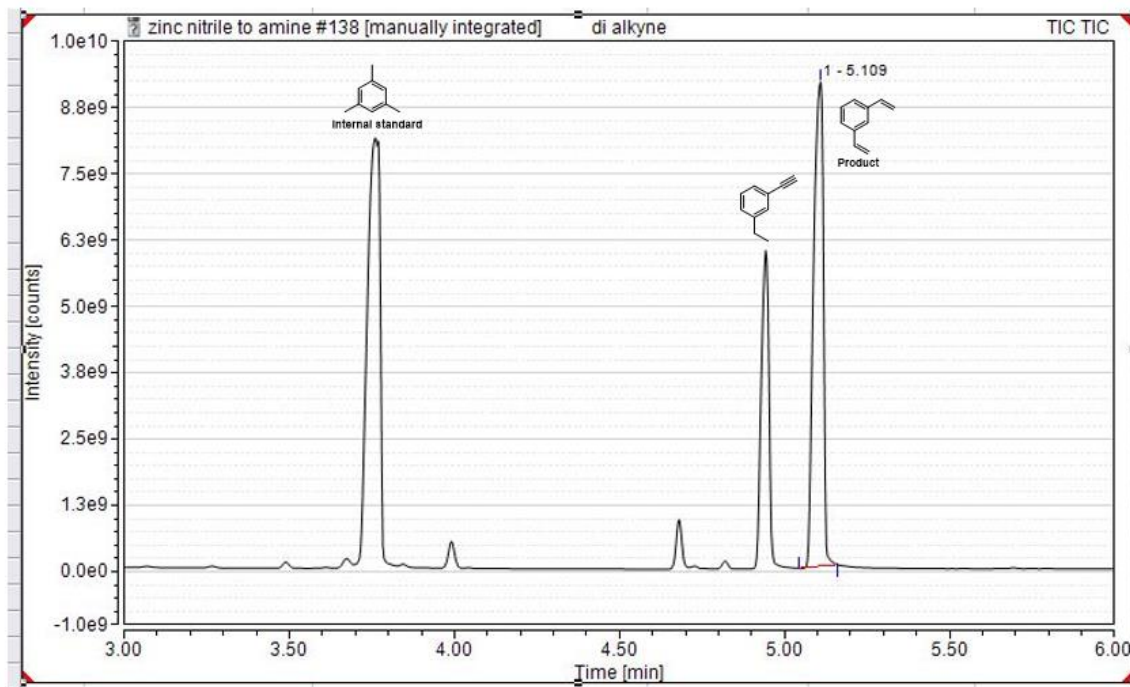
Peak Report

Peak	Retention Time (min)	Peak Area	Name
1	5.99	195792051	3-vinylbenzonitrile
2	3.77	355449089	Mesitylene

ESI-MS Spectra of 3-vinylbenzonitrile



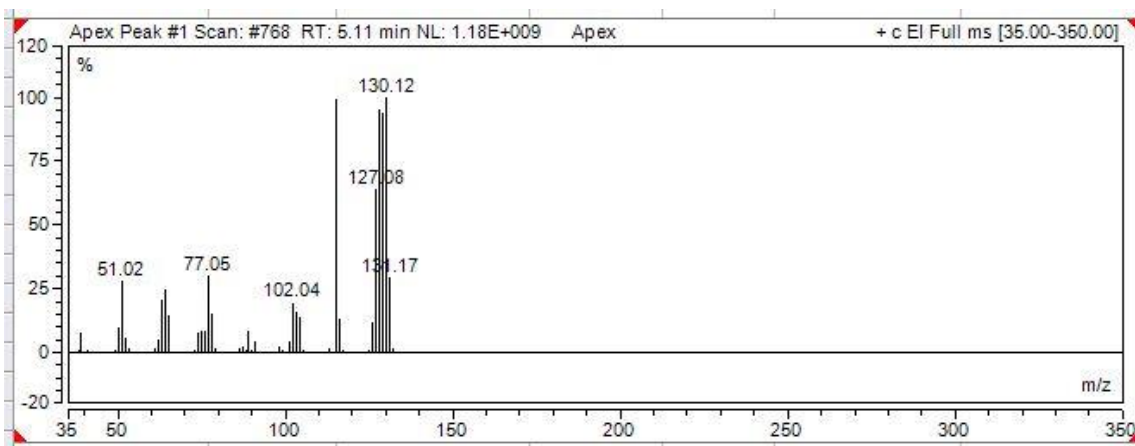
(x) GC Chromatogram of the reaction mixture of compound 2j:



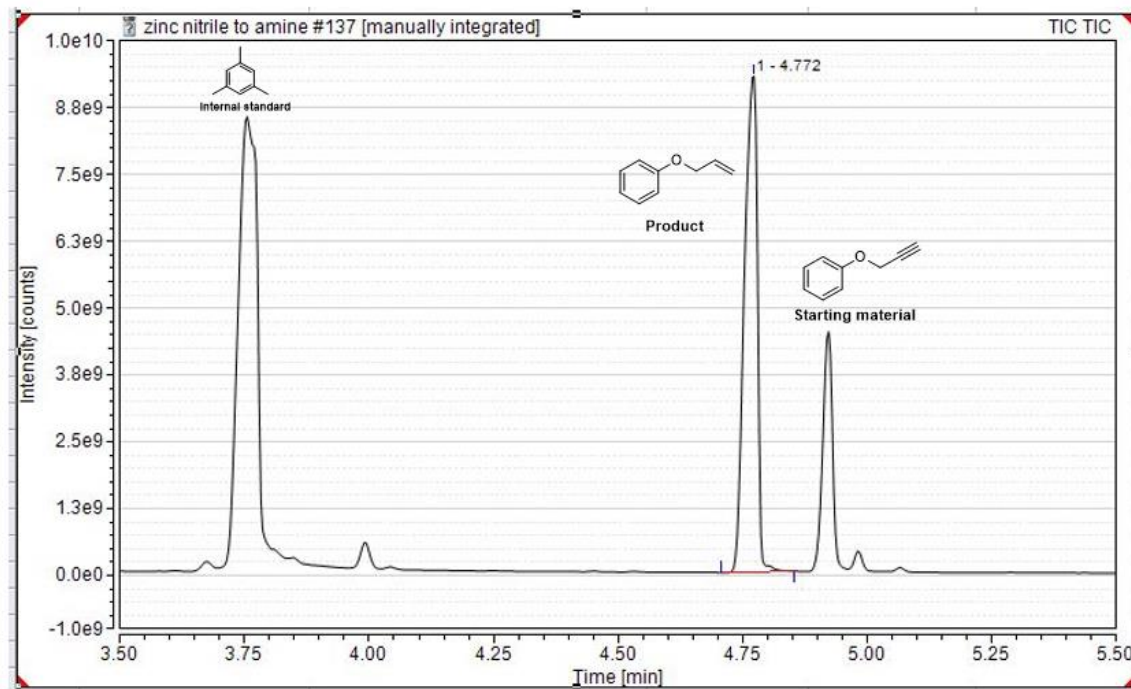
Peak Report

Peak	Retention Time (min)	Peak Area	Name
1	5.11	305883633	1,3-divinylbnzene
2	3.77	350314212	Mesitylene

ESI-MS Spectra of 1,3-divinylbnzene



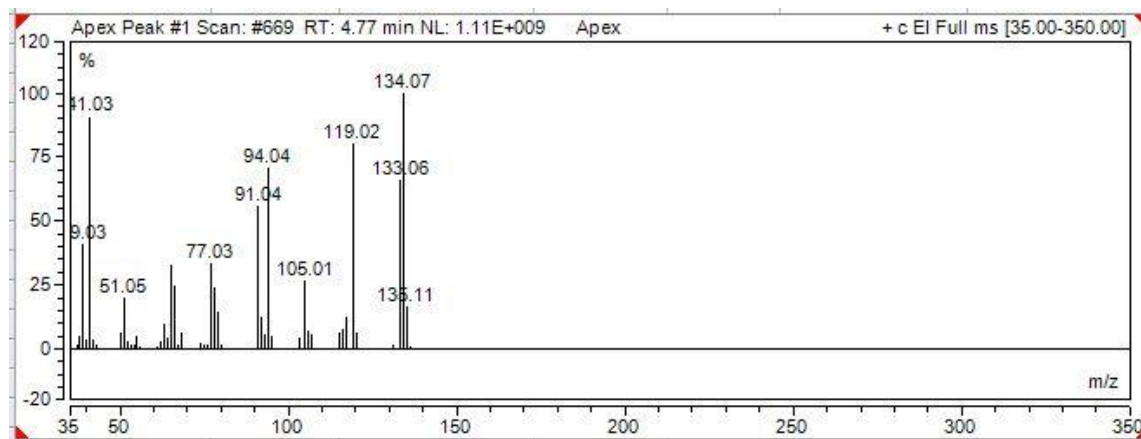
(xi) GC Chromatogram of the reaction mixture of compound 2k:



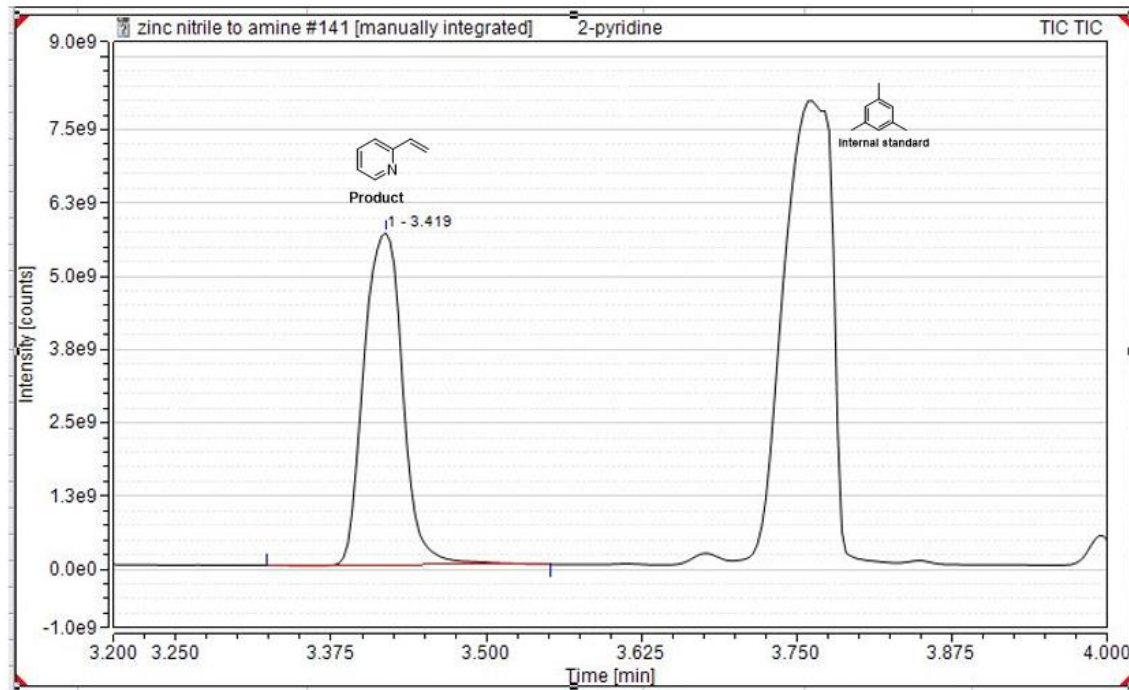
Peak Report

Peak	Retention Time (min)	Peak Area	Name
1	4.77	277495890	Allyl phenyl ether
2	3.77	350314212	Mesitylene

ESI-MS Spectra of Allyl phenyl ether



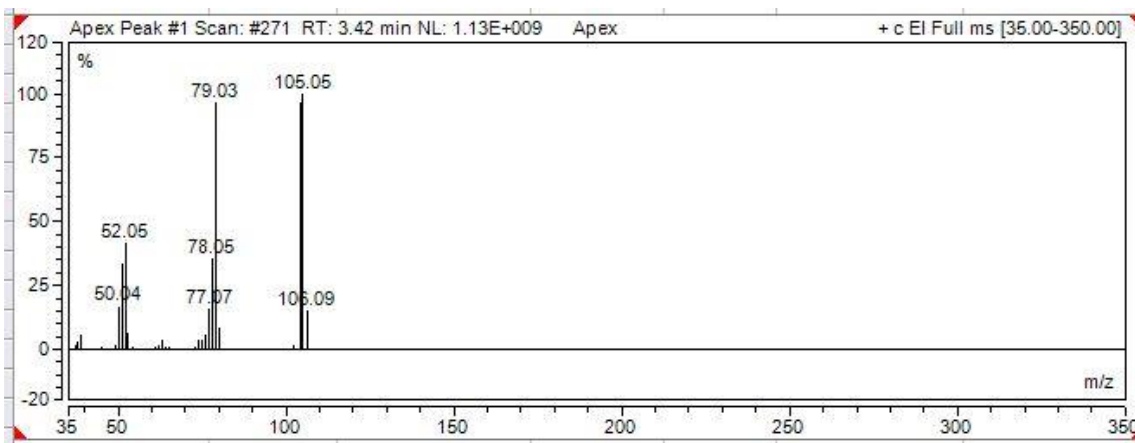
(xii) GC Chromatogram of the reaction mixture of compound 2l:



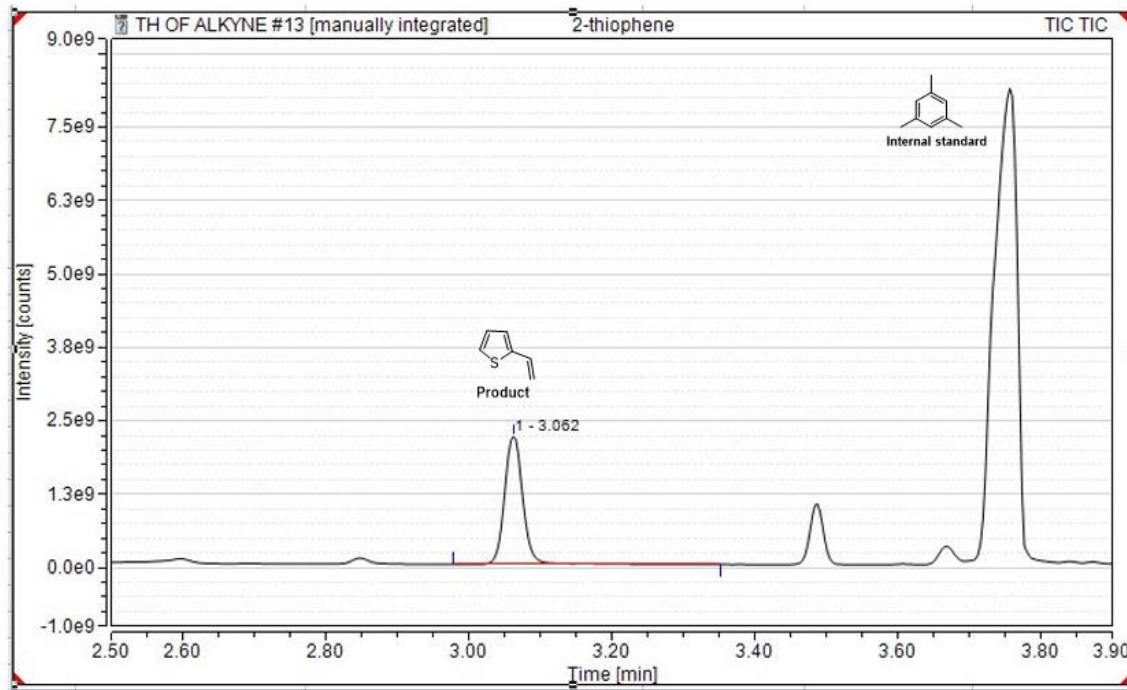
Peak Report

Peak	Retention Time (min)	Peak Area	Name
1	3.42	206977381	2-Vinylpyridine
2	3.77	306490750	Mesitylene

ESI-MS Spectra of 2-Vinylpyridine



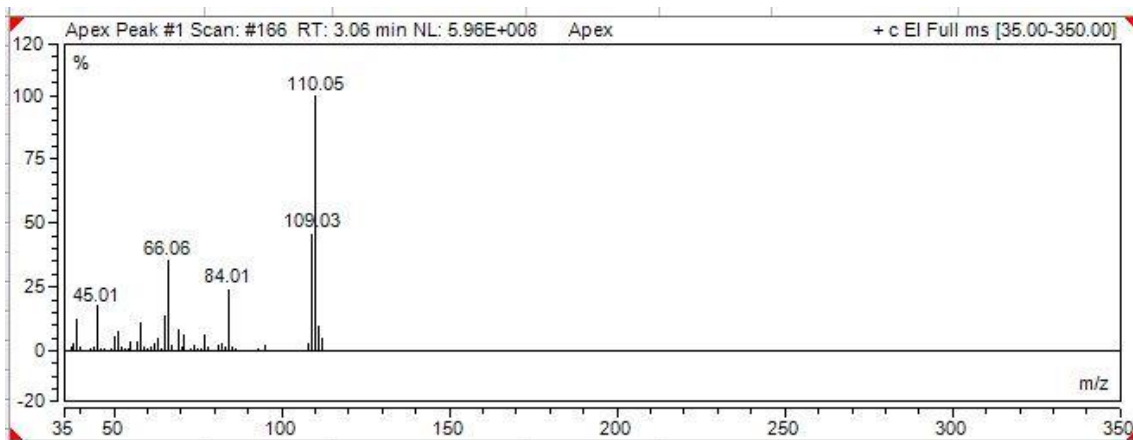
(xiii) GC Chromatogram of the reaction mixture of compound 2m:



Peak Report

Peak	Retention Time (min)	Peak Area	Name
1	3.06	63998245	2-Vinylthiophene
2	3.77	291872416	Mesitylene

ESI-MS Spectra of 2-Vinylthiophene



10. Crystallographic information of Fe-1 complex

The single crystals of **Fe-1** complex were obtained in DCM solution of **Fe-1** layering with hexane. The single crystal X-ray diffraction measurements were performed to determine the crystal structure at 100 K using APEX3 (Bruker, 2016; Bruker D8 VENTURE Kappa Duo PHOTON II CPAD) diffractometer having graphite-monochromatized (MoK α (0.71073)). The X-ray generator was operated at 50 kV and 30 mA. A preliminary set of unit cell parameters and an orientation matrix were calculated from 36 frames, and the cell refinement was performed by SAINT-Plus (Bruker, 2016). An optimized strategy used for data collection consisted of different sets of φ and ω scans with 0.5° steps φ/ω . The data were collected with a time frame of 10 sec by setting the sample to detector distance fixed at 40 cm. All the data points were corrected for Lorentzian, polarization, and absorption effects using SAINT-Plus and SADABS programs (Bruker, 2016). SHELXS-97 (Sheldrick, 2008) was used for structure solution, and full-matrix least-squares refinement on F^2 .^{3,4} The molecular graphics of ORTEP diagrams were performed by Mercury software. The crystal symmetry of the components was cross-checked by running the cif files through PLATON (Spek, 2020) software and notified that no additional symmetry was observed. The Encifer software was used to correct the cif files.

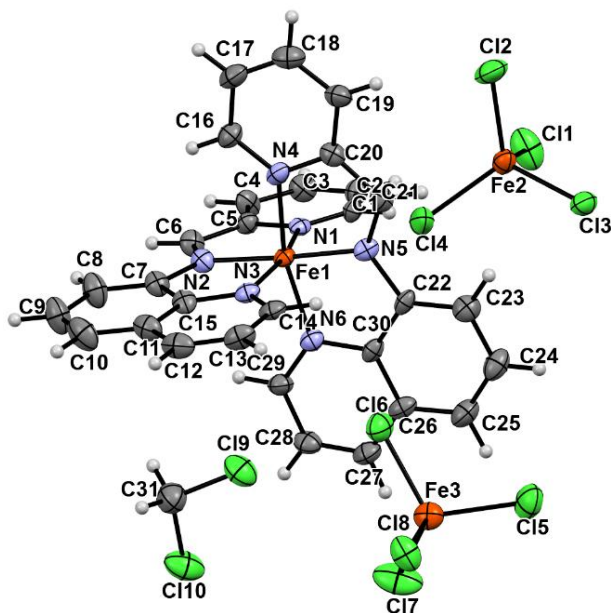


Figure S11. ORTEP diagram of compound **Fe-1**, the asymmetric unit contains one molecule of Fe^{+2} complex along with two FeCl_4 counter ions and one molecule of Dichloromethane solvent. Herein, the ellipsoids are drawn with a 50% probability.

Table S1. Crystallographic information details of compound **Fe-1** complex.

Crystal data	Fe-1 Complex
Chemical formula	C ₃₀ H ₂₂ FeN ₆ ·CH ₂ Cl ₂ ·2(Cl ₄ Fe)
Formula weight (M _r)	1002.61
Crystal system	Monoclinic
Space group	<i>P2₁/c</i>
Temperature T (K)	100
a (Å)	10.346 (6)
b (Å)	8.963 (5)
c (Å)	42.27 (2)
α (°)	90
β (°)	94.20 (3)
γ (°)	90
Z	4
Volume (Å ³)	3909 (4)
Source of radiation	MoKα (0.71073)
D _{calc} (g cm ⁻³)	1.704
Crystal size (mm)	0.19×0.1×0.09
μ (mm ⁻¹)	1.82
Data collection	
Diffractometer	Bruker D8 VENTURE Kappa Duo PHOTON II CPAD
Absorption correction	Multi-scan (SADABS; Bruker, 2016)
T _{min} , T _{max}	0.6008, 0.7456
No. of measured, independent and observed [I > 2+σ(I)] reflections	111709, 8514, 6288

Theta range (°)	2.133-27.000
R _{int}	0.129
Refinement	
R[F ² > 2σ (F ²)], wR(F ²)	0.082, 0.166
GOF on F ²	1.13
No. of independent reflections	8514
No. of parameters	451
F ₀₀₀	2000
No. of restraints	0
H-atom treatment	Constr
Δρ _{max} , Δρ _{min} (e Å ⁻³)	0.99, -0.69
CCDC number	2271237

Table S2. Bond Distances (Å).

Bond	Distance (Å)	Bond	Distance (Å)
Fe1-N1	1.9714(11)	C1-C2	1.3853(8)
Fe1-N2	1.8880(11)	C2-C3	1.3798(8)
Fe1-N3	1.9597(11)	C3-C4	1.3671(8)
Fe1-N4	1.9680(11)	C4-C5	1.3809(8)
Fe1-N5	1.8936(11)	C5-C6	1.4560(8)
Fe1-N6	1.9622(11)	C7-C15	1.4218(8)
Fe2-Cl2	2.2014(13)	C7-C8	1.3708(8)
Fe2-Cl3	2.1959(13)	C8-C9	1.4069(8)
Fe2-Cl4	2.1979(13)	C9-C10	1.3671(8)
Fe2-Cl1	2.1783(13)	C10-C11	1.4299(8)
Fe3-Cl6	2.2047(13)	C11-C12	1.4164(8)

Fe3-C17	2.1801(13)	C11-C15	1.4146(8)
Fe3-C15	2.1901(13)	C12-C13	1.3527(8)
Fe3-C18	2.2080(13)	C13-C14	1.4129(8)
C19-C31	1.7495(10)	C16-C17	1.4045(8)
C110-C31	1.7722(10)	C17-C18	1.3832(8)
N1-C1	1.3253(8)	C18-C19	1.3645(8)
N1-C5	1.3728(8)	C19-C20	1.4072(8)
N2-C6	1.3068(8)	C20-C21	1.4338(8)
N2-C7	1.4173(8)	C22-C30	1.4042(8)
N3-C14	1.3172(8)	C22-C23	1.3716(8)
N3-C15	1.3830(8)	C23-C24	1.4049(8)
N4-C20	1.3730(8)	C24-C25	1.3713(8)
N4-C16	1.3332(8)	C25-C26	1.4043(8)
N5-C22	1.4314(8)	C26-C27	1.3965(8)
N5-C21	1.2980(8)	C26-C30	1.4257(8)
N6-C29	1.3338(8)	C27-C28	1.3478(8)
N6-C30	1.3754(8)	C28-C29	1.4160(8)
C1-H1	0.950	C17-H17	0.950
C2-H2	0.950	C18-H18	0.950
C3-H3	0.950	C19-H19	0.950
C4-H4	0.950	C21-H21	0.950
C6-H6	0.950	C23-H23	0.950
C8-H8	0.950	C24-H24	0.950
C9-H9	0.950	C25-H25	0.950
C10-H10	0.950	C27-H27	0.950
C12-H12	0.950	C28-H28	0.950
C13-H13	0.950	C29-H29	0.950

C14-H14	0.950	C31-H31A	0.990
C16-H16	0.950	C3-H31B	0.990

Table S3. Bond Angles (°)

Bond	Angles (°)	Bond	Angles (°)
N1-Fe1-N2	81.49(3)	Fe1-N1-C5	113.44(3)
N1-Fe1-N3	164.67(3)	C1-N1-C5	116.89(3)
N1-Fe1-N4	93.71(3)	Fe1-N2-C7	116.63(3)
N1-Fe1-N5	97.59(3)	C6-N2-C7	125.07(3)
N1-Fe1-N6	90.21(3)	Fe1-N2-C6	118.29(3)
N2-Fe1-N3	83.39(3)	Fe1-N3-C14	130.88(3)
N2-Fe1-N4	96.22(3)	Fe1-N3-C15	111.91(3)
N2-Fe1-N5	177.21(3)	C14-N3-C15	117.18(3)
N2-Fe1-N6	98.84(3)	C16-N4-C20	118.57(3)
N3-Fe1-N4	90.47(3)	Fe1-N4-C20	112.50(3)
N3-Fe1-N5	97.62(3)	Fe1-N4-C16	128.92(3)
N3-Fe1-N6	89.56(3)	Fe1-N5-C22	114.91(3)
N4-Fe1-N5	81.18(3)	Fe1-N5-C21	118.69(3)
N4-Fe1-N6	164.84(3)	C21-N5-C22	126.39(3)
N5-Fe1-N6	83.79(3)	C29-N6-C30	118.92(3)
Cl1-Fe2-Cl3	105.53(3)	Fe1-N6-C29	129.15(3)
Cl1-Fe2-Cl4	108.45(3)	Fe1-N6-C30	111.90(3)
Cl2-Fe2-Cl3	112.73(3)	N1-C1-C2	123.11(3)
Cl2-Fe2-Cl4	107.83(3)	C1-C2-C3	119.33(3)
Cl3-Fe2-Cl4	110.23(3)	C2-C3-C4	118.88(3)
Cl1-Fe2-Cl2	112.01(3)	C3-C4-C5	119.04(3)
Cl5-Fe3-Cl6	110.27(3)	C4-C5-C6	124.56(3)

Cl5-Fe3-Cl7	110.60(3)	N1-C5-C4	122.72(3)
Cl6-Fe3-Cl7	109.08(3)	N1-C5-C6	112.72(3)
Cl6-Fe3-Cl8	107.42(3)	N2-C6-C5	114.05(3)
Cl7-Fe3-Cl8	110.54(3)	C8-C7-C15	121.38(3)
Cl5-Fe3-Cl8	108.88(3)	N2-C7-C15	110.66(3)
Fe1-N1-C1	129.64(3)	N2-C7-C8	127.95(3)
C7-C8-C9	118.69(3)	C25-C26-C27	125.84(3)
C8-C9-C10	121.19(3)	C26-C27-C28	121.17(3)
C9-C10-C11	121.82(3)	C27-C28-C29	119.31(3)
C10-C11-C12	126.04(3)	N6-C29-C28	121.94(3)
C12-C11-C15	117.33(3)	N6-C30-C22	117.46(3)
C10-C11-C15	116.63(3)	N6-C30-C26	121.41(3)
C11-C12-C13	120.16(3)	C22-C30-C26	121.13(3)
C12-C13-C14	118.64(3)	N1-C1-H1	118
N3-C14-C13	124.35(3)	C2-C1-H1	118
N3-C15-C7	117.38(3)	C3-C2-H2	120
N3-C15-C11	122.33(3)	C1-C2-H2	120
C7-C15-C11	120.29(3)	C2-C3-H3	121
N4-C16-C17	121.81(3)	C4-C3-H3	121
C16-C17-C18	119.19(3)	C3-C4-H4	120
C17-C18-C19	120.07(3)	C5-C4-H4	120
C18-C19-C20	118.53(3)	C5-C6-H6	123
C19-C20-C21	123.96(3)	N2-C6-H6	123
N4-C20-C19	121.81(3)	C9-C8-H8	121
N4-C20-C21	114.24(3)	C7-C8-H8	121
N5-C21-C20	113.37(3)	C8-C9-H9	119
C23-C22-C30	119.95(3)	C10-C9-H9	119

N5-C22-C23	128.07(3)	C11-C10-H10	119
N5-C22-C30	111.93(3)	C9-C10-H10	119
C22-C23-C24	119.41(3)	C11-C12-H12	120
C23-C24-C25	121.20(3)	C13-C12-H12	120
C24-C25-C26	121.20(3)	C12-C13-H13	121
C25-C26-C30	116.96(3)	C14-C13-H13	121
C27-C26-C30	117.20(3)	N3-C14-H14	118
C13-C14-H14	118	C24-C25-H25	119
C17-C16-H16	119	C26-C25-H25	119
N4-C16-H16	119	C26-C27-H27	119
C16-C17-H17	120	C28-C27-H27	119
C18-C17-H17	120	C27-C28-H28	120
C19-C18-H18	120	C29-C28-H28	120
C17-C18 -H18	120	C28-C29-H29	119
C18-C19-H19	121	N6-C29-H29	119
C20-C19-H19	121	C19-C31-C110	111.32(3)
N5-C21-H21	123	C19-C31-H31A	109
C20-C21-H21	123	C19-C31-H31B	109
C24-C23-H23	120	C110-C31-H31A	109
C22 -C23-H23	120	C110-C31-H31B	109
C23-C24-H24	119	H31A-C31-H31B	108
C25-C24-H24	119		

Table S4. Hydrogen-bond geometry (Å° and $^\circ$) of **Fe-1** complex are given as below:

Name of the compound	$D-H\cdots A$	$D-H$	$H\cdots A$	$D\cdots A$	$D-H\cdots A$
Fe-1	C2-H2 \cdots C11	0.950	2.690	3.532(2)	148
	C10-H10 \cdots C17	0.950	2.810	3.678(2)	153
	C21-H21 \cdots C14	0.950	2.790	3.719(2)	168
	C29-H29 \cdots C18	0.950	2.760	3.615(2)	150

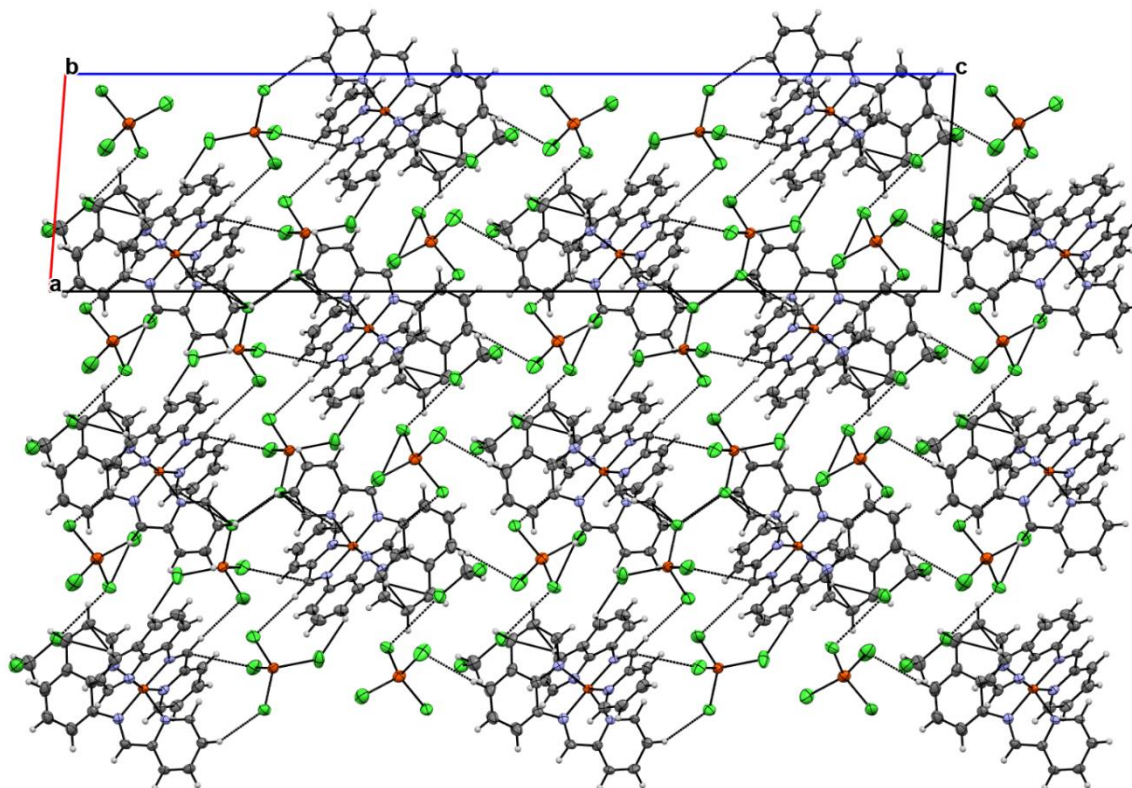


Figure S12. Crystal packing of **Fe-1** complex.

11. Copies of ^1H and $^{13}\text{C}\{^1\text{H}\}$ NMR Spectra of the isolated products:

^1H and $^{13}\text{C}\{^1\text{H}\}$ NMR spectra of **2a**:

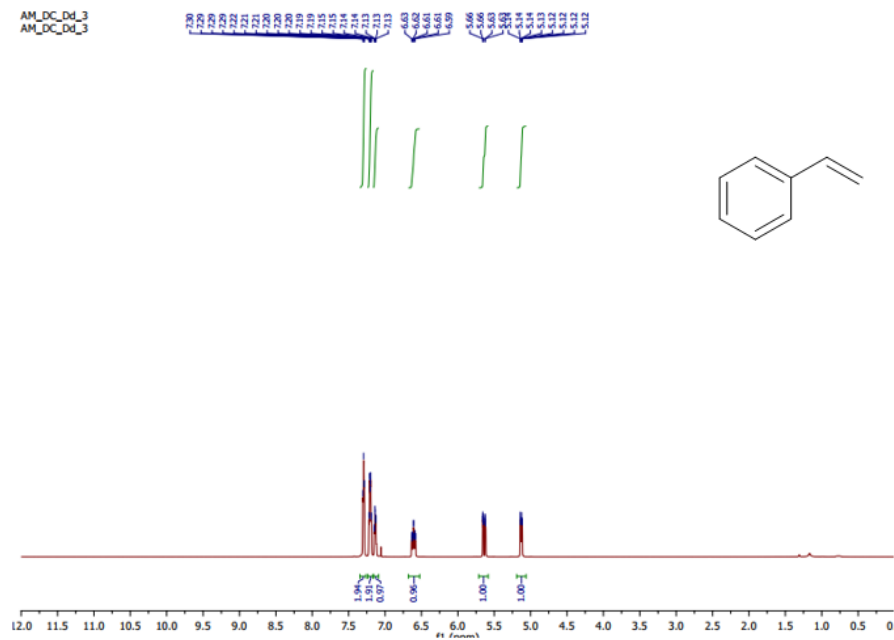


Figure S13. ^1H spectrum (600 MHz) of **2a** in CDCl_3 .

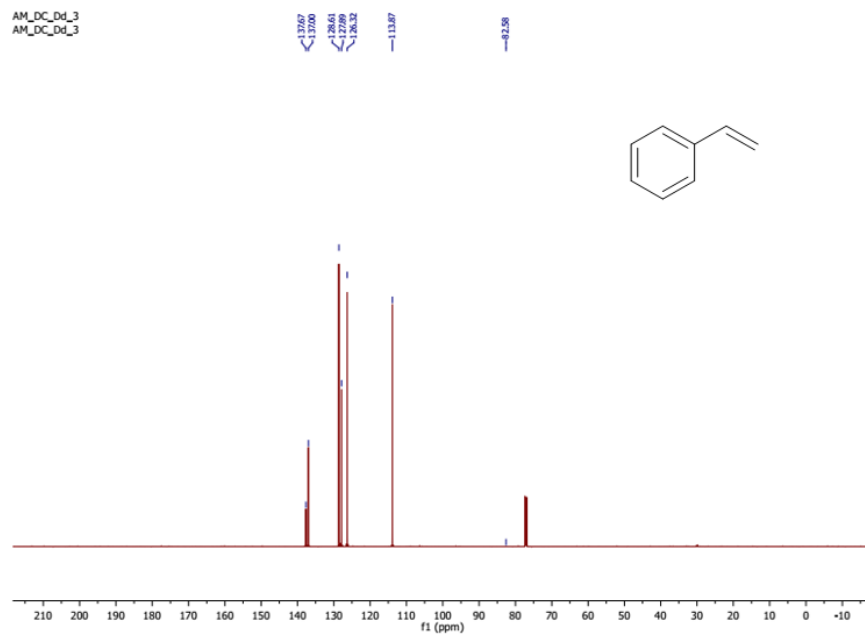


Figure S14. $^{13}\text{C}\{^1\text{H}\}$ spectrum (125 MHz) of **2a** in CDCl_3 .

^1H and $^{13}\text{C}\{^1\text{H}\}$ NMR spectra of **2b:**

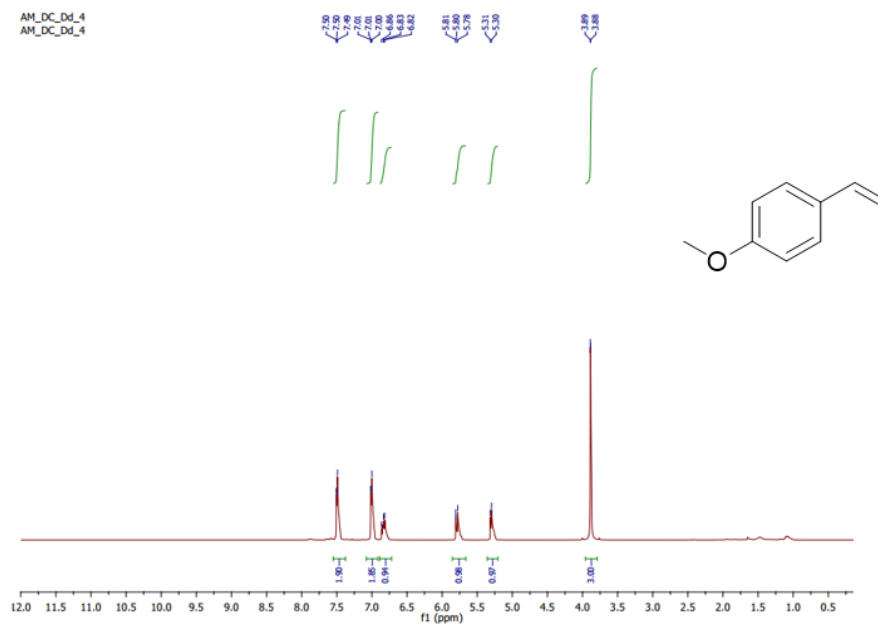


Figure S15. ^1H spectrum (600 MHz) of **2b** in CDCl_3 .

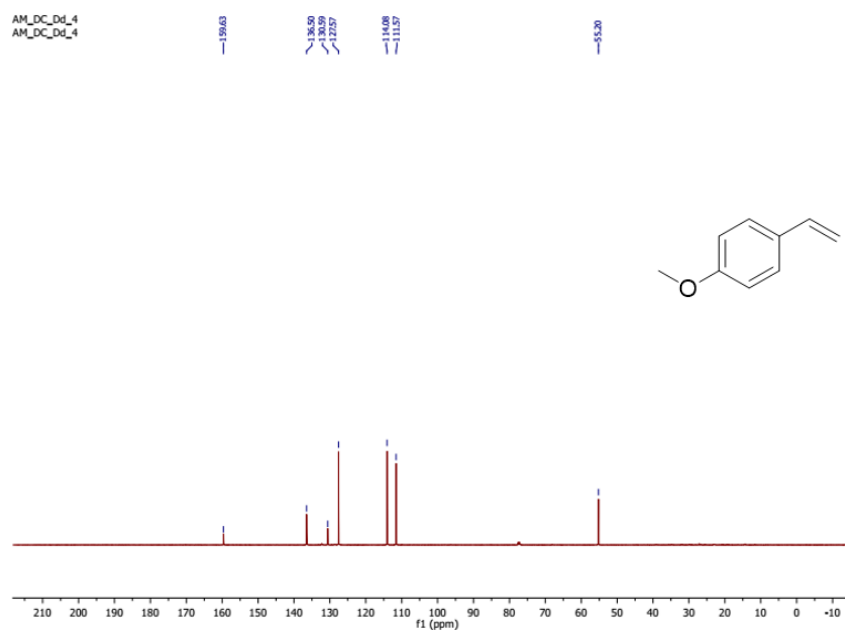


Figure S16. $^{13}\text{C}\{^1\text{H}\}$ spectrum (125 MHz) of **2b** in CDCl_3 .

12. References:

- (1) N. Podder, S. Mandal, *New J. Chem.*, 2020, **44**, 12793-12805.
- (2) Q. Liu, L. Yang, C. Yao, J. Geng, Y. Wu, X. Hu, *Org. Lett.* 2021, **23**, 3685-3690.
- (3) G. M. Sheldrick, Crystal structure refinement with SHELXL, *Acta Cryst.*, 2015, **C71**, 3-8.
- (4) G. M. Sheldrick, SHELXT - Integrated space-group and crystal-structure determination, *Acta Cryst.*, 2015, **A71**, 3-8.